

## Response to Anonymous Referee #1

Dear editor,

We would like to thank the first referee for his/her clearly positive comments that help us improve our manuscript. We replied to the comments of referee#1 in detail and explained how we have modified the manuscript for publication in Biogeosciences. Referee's comments are shown in black and our responses are shown in blue.

### Anonymous Referee #1

«Overall comments» In general, I feel positive about the overall contribution of the paper. The topic is interesting and relevant to the goal of Biogeosciences. The approaches that the authors adopted are interdisciplinary and provide educative information to this topic. The data and interpretation are mostly convincing with several points that I request for further clarification (see comments below). The authors need to improve the presentation a lot as figure 2 is hard to read, some of the references cited are out of date, a few sentences are quite awkward to read, and Table 2 needs more polishing. I've included my detail suggestions for these technical issues in the pdf file. Despite these minor flaws, I strongly encourage to publish this paper after all of my concerns are addressed.

«Detail comments» My major concerns about the paper are as follow: for analytical and model approach-

1) In quite a few of samples, the sulfate concentrations are over seawater value (28mM). The authors explained this as dissolution of anhydrite. The alternative explanation will be re-oxidation of hydrogen sulfide in the porewater samples after they were collected. In the sampling procedure the authors described, I do not see any description such as flushing the porewater samples with N<sub>2</sub> gas or fixing sulfide with Zn(OAc)<sub>2</sub> solution to get rid of sulfide. Some clarification about how this is of concern should be addressed.

### Response:

All of the samples were processed inside an anaerobic glove bag with N<sub>2</sub> atmosphere. We added this information to the paper. However the reviewer is correct that it may be possible that some H<sub>2</sub>S is oxidized in the shallow subsurface of the cores due to oxygen penetration due to bioturbation.

Therefore, excess sulfate could potentially be from H<sub>2</sub>S oxidation and/or from sulfate input from groundwater. We note that in this specific site groundwater has been previously identified as a source of excess sulfate and excess Sr. Regardless we now include the option of H<sub>2</sub>S oxidation in the revised manuscript, whilst further noting that, since R<sub>SD</sub> is the net sulfate depletion, model results may underestimate the true R<sub>POC</sub> and R<sub>M</sub> due to sulfide oxidation. However, this is only relevant for very few cores in Group-1 and Group-2 where a shallow subsurface excess sulfate is observed. Although we mention this option for completion we believe that groundwater input is

a more likely source due to correlation between excess sulfate and excess Sr which has been previously described and is consistent with groundwater input.

Perry et al. (2002) identified dissolution of evaporites within the freshwater lens as the probable source of the excess  $\text{SO}_4^{2-}$  found in some Yucatán groundwater by using the ratio between sulfate and chloride ( $100 \times (\text{SO}_4/\text{Cl})$ ). Ratios higher than seawater (average seawater is 10.3) are expected where gypsum/anhydrite dissolution is involved (Perry et al. 2002). The other indicator is Sr/Cl ratio which in groundwater is invariably higher than the seawater value and indicates dissolution of celestite (from evaporite) and/or aragonite (Perry et al. 2002). The region east and south of Lake Chichancanab, Mexico, referred to as the Evaporite Region by Perry et al. (2002) is characterized by distinctive topography and the high-sulfate content of groundwater (Perry et al. 2002). The groundwater from the presumed source region, Lake Chichancanab, flows northward into the Celestún Estuary which can be recognized by the progressive decrease in the ratio  $[\text{SO}_4/\text{Cl}]_{\text{groundwater}}/[\text{SO}_4/\text{Cl}]_{\text{seawater}}$  in water from southeast to northwest (Perry et al., 2009). These parameters in Celestún lagoon published in Young et al., (2008) are consistent with our interpretation that gypsum/anhydrite dissolution involved in the groundwater contributes to Celestún lagoon.

2) The authors modeled the system for 1 Myr to reach steady state. I wonder if this is a reasonable assumption to make in this case? From the high sedimentation rate (0.25- 0.35 cm/yr) of these cores, the age of the sediments investigated is not older than several years. Besides, this environment must be very dynamic with episodic input of water from different sources, bioturbation, and even sediment reworking. Why not simulate the system only to their real age, say 1-5 years? I believe this will significantly impact the results.

Response:

Yes, it's true that this is a very dynamic study area. Below in Fig R1 we show the example of modeling with 1 yr and 5 yr simulations for core 1CEL\_Oct01. The results are the same as the 1 Myr simulations which means this dataset has reached steady state within 1 yr or less and using longer time scales does not make a difference.

Specifically we note that the long simulation time of 1 Myr is a default setting in this version of the model to ensure that the results for all cores are under steady state. However, we see the possible confusion. The 5 year simulation time now reported can be justified using the following equation (Boudreau, 1997):

$$t = \frac{L^2}{2 \times D_M}$$

where t is time, L is the distance involved in a typical diffusive movement (length of the model column) and  $D_M$  is the molecular diffusion coefficient. The time for methane and sulfate diffusion over the length of modeled sediments (20 cm) is less than 0.6 yr ( $D_{\text{M}(\text{CH}_4)} = 659 \text{ (cm}^2 \text{ yr}^{-1})$  and  $D_{\text{M}(\text{SO}_4^{2-})} = 382 \text{ (cm}^2 \text{ yr}^{-1})$  for e.g. core 1CEL\_Oct01). Now we show the data using 5 years as the time needed for steady state and changed the text and figures accordingly. This makes no difference to the results.

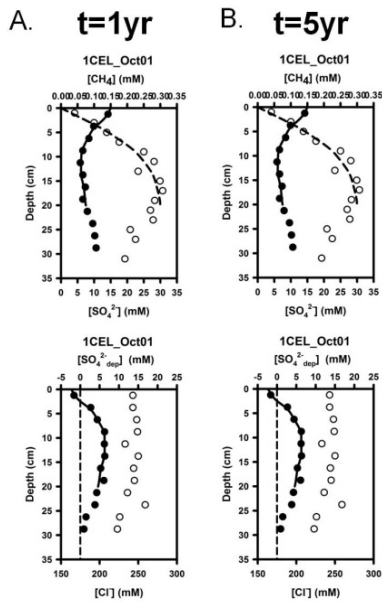


Fig. R1: Depth profiles for modeled (lines) and measured/calculated (symbols) concentration of dissolved methane (dashed line; open circle), sulfate (solid line; solid circle) in the upper panel and sulfate depletion (solid line; solid circle), zero sulfate depletion (dashed line) and chloride (open circle) in the lower panel for core 1CEL\_Oct01 for: (A) 1yr and (B) 5yr simulation times.

3) I find it difficult to understand the reactions described in the appendix:

a. Page17931, line20-22: “Since AOM may play a minor role in the methane and sulfate rich sediment and RAOM was included in the net reaction rates of methane and sulfate this is justified.” I don’t understand at all what does this sentence mean. AOM should play an important role when you have abundant methane and sulfate isn’t? What is justified? By what?

Response:

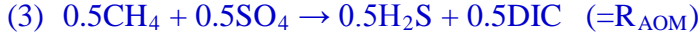
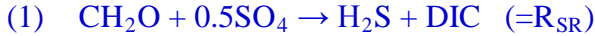
We have now simplified the model set-up because, based on our data, we cannot accurately quantify the relative proportion of sulfate loss due to organoclastic sulfate reduction and AOM. The sentence pointed out by the reviewer was unclear and has been removed.

b. Eq. A6: so you exclude entirely AOM when SO<sub>4</sub>-dep is positive? I thought SO<sub>4</sub>-dep>0 means active removal of sulfate? Not by AOM?

Response:

SO<sub>4</sub>-dep>0 means that active removal of sulfate is dominated by organoclastic sulfate reduction, although R<sub>SD</sub> includes R<sub>SR</sub> and R<sub>AOM</sub>. Since we can see evidence for methane production along with sulfate reduction in many of our sites especially cores in Group-1 and Group-2, we use the rate derived from [SO<sub>4</sub><sup>2-</sup><sub>dep</sub>] profile (R<sub>SD</sub>) to represent the rate of organoclastic sulfate reduction (R<sub>SR</sub>).

In the sulfate reduction zone, we assume the co-occurrence of the following reactions:



In the reaction stoichiometry,  $R_{\text{SR}}$  in reaction (1) is  $0.5R_{\text{POC}}$ . In terms of net sulfate reaction,  $R_{\text{SD}}=R_{\text{SR}}+R_{\text{AOM}}$ . Since the 3 reactions are coupled in the sulfate reduction zone and reaction (2) + reaction (3) is equal to reaction (1), this means that  $R_{\text{SD}}=0.5R_{\text{POC}}$ . Hence,  $R_{\text{AOM}}$  is negligible compared with  $R_{\text{SR}}$  for  $R_{\text{SD}}$ . We have revised the equations for  $R_{\text{SD}}=R_{\text{SR}}+R_{\text{AOM}}=R_{\text{SR}}=0.5R_{\text{POC}}$ . To estimate the fraction of organic matter degradation via methanogenesis ( $R_{\text{M}}$ ) and organoclastic sulfate reduction ( $R_{\text{SR}}$ ), Michaelis-Menten kinetic limitation term used for methanogenesis ( $R_{\text{M}}$ ) and organoclastic sulfate reduction ( $R_{\text{SR}}$ ) are expressed as:

$$R_{\text{SR}} = 0.5 \cdot R_{\text{POC}} \cdot f_{\text{SO}_4^{2-}}$$

$$R_{\text{M}} = 0.5 \cdot R_{\text{POC}} \cdot (1 - f_{\text{SO}_4^{2-}})$$

AOM may occur in these systems, but the data and model sensitivity results indicate that it is insufficient to prevent  $\text{CH}_4$  escape to the bottom water, probably because of the abundant organic matter available for sulfate reducers to use instead of  $\text{CH}_4$ . We have revised this in the manuscript.

d. Eq. A7: I understand you related  $R_{\text{poc}}$  to  $R_{\text{sr}}$  assuming all sulfate reduction is organoclastically. Again, is this a good assumption? What's the role of AOM in sulfate reduction? I think you are right that organoclastic SR is important here but you need to explain this better.

Response:

AOM plays a minor role in sulfate reduction. Please see the response to comments (3).

e. Eq. A12: How does  $R_{\text{corganic}}$  different from  $R_{\text{poc}}$ ? How does the comparison of these two rates like? From table 2, I see them can be orders of magnitude different (e.g. 1CH\_Dec00). Why?

Response:

The reason we simulate  $[\text{SO}_4^{2-}]_{\text{dep}}$  profiles to derive rates of organic matter degradation, organoclastic sulfate reduction and methanogenesis is because measured organic matter contents in this area show evidence for a change in depositional regime over time (Gonnea et al., 2004,

and Fig. 4 in this version). Organic matter cannot therefore be used for accurate organic matter degradation calculations. To avoid the confusion between  $R_{\text{organic}}$  and  $R_{\text{POC}}$ , we have removed the sampling and analytical methods, results, discussions and the model equation related to the measured organic contents from our manuscript and refer to measured organic matter contents from Gonnea et al (2004) and Eagle (2002, thesis).

This is stated more clearly in the revised manuscript.

4) Refer back to my comment (2), time scale of your model is really important. It determines the scale of your kinetic constants. For example, you use 0.01 1/yr for your  $k_{\text{corg}}$ . It may be a lot different if you only run the model for 5 years and. for scientific interpretation/discussion- I think the experiment and model results support most of the interpretation by the authors. I however feel that the authors should extend the discussion a bit more from the following prospects:

1) Maybe my biggest concern for the paper is the assumption of steady state. The authors should provide good reasons why they think this assumption is adequate as the system is so dynamic.

Response:

Please see the response to comment (2). We are now running the model for 5 years to reach steady state (see comment above). We use a steady state model because we do not have enough data to constrain a dynamic model such as regular monitoring of porewater sulfate, methane and chloride concentrations. The steady state model is still useful because we apply it to a wide range of profile types which represent the different conditions in the system and capture the system dynamics.

2) The authors presented tremendous amount of temporal/spatial porewater data in this paper but did not spend much effort in discussing these. The grouping of data is based on the shape of profiles and thus their dominate reactions. Do these groups correspond to any particular location or season that might explain the such dominance in terms of biogeochemistry?

Response:

We have included additional discussion to show there is no relation between profile time and location or season and that the variability is a result of the system being heterogeneous and probably highly dynamic. We do not have sufficient data to differentiate between temporal and spatial trends, however as we show cores collected at the same time close to each other may differ and cores collected at the same sites during different times also differ from each other hence we believe that if we monitored any one site continuously it is likely that all profile types will be captured at one site.

3) Results from incubation experiments are one of the highlights in this paper but the authors only mentioned it briefly in 5.1 section. I wonder are the authors able to derive some rates from the experiments that can be compared with the rates estimated by modeling. Also, how do all these rates compared to other similar environments? I feel like the authors should put their results in a larger global context to reveal the significance of their data.

Response:

Yes, we are able to derive some rates from the experiments which have been added to Table 1 in the manuscript. An additional table (Table 3) includes rates estimated by modeling which can be used to compare with the rates from the experiments.

The maximum methane production rates listed in Table 1 from TMA, methanol and H<sub>2</sub> treatments are higher than the methane production rates from coastal freshwater and brackish wetland sediments which were measured using radiolabeled acetate and bicarbonate in slurries and reported in Segarra et al. (2013).

In addition to depth-integrated rates, Table 3 listed model derived maximum methanogenesis (Max-RM), sulfate reduction and AOM rates (Max-R<sub>SR</sub>). Maximum methane production rates estimated from TMA, methanol and H<sub>2</sub> treatments of sediment slurry incubations (Table 1) are similar to values reported by model derived Max-RM at station 16CEL (Table 3) the site from which sediments were collected for sediment slurry incubations. Model derived Max-RM in some cores can reach to 1-2 orders of magnitude higher than rates derived from the sediment slurry incubations (e.g., cores 1CEL\_Jul02, 1\_1CH\_Oct01, 2CEL\_Oct01 and 14CEL\_Dec00). Although our model results show that organoclastic sulfate reduction dominates organic matter degradation, model derived Max-RM are even higher than the maximum sulfate reduction rates in cores 1\_1CH\_Oct01 and 1\_2CH\_Oct01. Methanogenesis rates in this study area are more important than in other mangrove systems where methanogenesis is negligible (e.g., Thailand, Kristensen et al., 2000; Malaysia, Alongi et al., 2004; Australia, Kristensen and Alongi, 2006).

We include this in the discussion section of the manuscript.

4) The authors introduced the different seasons of this area and the potential impact to the sediment and porewater systems. However, I do not see further discussion about how their results reflect such seasonality. I feel a great pity that the authors did not translate the “numbers” they got from their modeling and experiments into something helpful to understand the spatial and temporal heterogeneity of the environment.

Response:

Model derived methane fluxes to the water column are listed in Table 2 ( $F_{\text{methane (top)}}$ ) and reveal that fluxes (0.011-21 mmol CH<sub>4</sub> m<sup>-2</sup> d<sup>-1</sup>) are similar or up to two orders of magnitude larger than fluxes reported for other mangrove systems in, e.g., Florida (0.02 mmol CH<sub>4</sub> m<sup>-2</sup> d<sup>-1</sup>, Barber et al., 1988; Harriss et al., 1988), Australia (0.03-0.52 mmol CH<sub>4</sub> m<sup>-2</sup> d<sup>-1</sup>, Kreuzwieser et al., 2003), and India (5.4-20.3 mmol CH<sub>4</sub> m<sup>-2</sup> d<sup>-1</sup>, Purvaja and Ramesh, 2001). Our values as well as the depth-integrated rates (Fig. 2) show no relation between sampling time and location or season. Since all of the different types of methane depth profiles (group-1, group-2, etc) were found during each sampling trip, and no obvious trends in spatial and temporal distribution (seasons and sampling locations) were observed, model derived methane effluxes to the water column and the variability in the porewater methane concentrations and depth-integrated turnover rates suggest a very dynamic system with high methane production and efflux rates.

We have included this in the discussion section of the manuscript.

«Minor/technical comments»

1) My biggest comments on the technical part of the paper is its presentation. The lead author tend to use long sentences with many clauses.

I would suggest split the long sentences into shorter ones which will be more understandable for readers who know nothing about modeling especially.

Response:

We have improved the English structure.

2) The authors also need to consider more recent literatures. When the hypothesis was built solely based on some 80' and 90' papers, it's hard not to think there may be different views in the current research.

Response:

More recent literature has been included.

3) The Figure 2 is small and difficult to read. You need to figure out a different way to present these.

Response:

Fig. 2 was moved to supplementary material and replaced with a figure showing one typical profile per group. All figure qualities were improved.

4) I have a few comments for Table 2. You need to be more careful about the significant digits. I don't think the model can give that many meaningful digits. The use of "F" at header row is confusing. I know you explain below but it is intuitionally awkward especially when you mixed the real fluxes with depth-integrated rates. The negative sulfate depletion rates and sulfate reduction rates are also awkward. It makes no physical sense unless you meant the reactions are reversible, which I think are not.

Response:

The table has been revised.

## **Response to Referee #2 (Dr. Pohlman)**

Dear editor,

We would like to thank the second referee, Dr. Pohlman, for his support of our manuscript and for giving us comments to improve the manuscript. We replied to his comments in detail point by point and explained how we have modified the manuscript for publication in Biogeosciences. Dr. Pohlman's comments are shown in black and our responses are shown in blue.

### General Comments:

The authors present sulfate, methane and chloride data from sediment cores collected from two coastal mangrove systems in the Yucatan Peninsula. The authors group the cores into 5 sets that generalize the sulfate and methane profile behavior. Because the analytical data are limited to concentration profiles of 3 constituents, they apply the Wallman et al. 2006 transport-reaction model to explain potential processes affecting the pore water geochemistry. An unusual and interesting observation is that methane and sulfate often coexist in the porewater, suggesting a non-competitive substrate (i.e., one used only by methanogens) allows methanogens to be active in the presence of sulfate reducers. A series of incubations that includes a treatment with the non-competitive substrates TMA and methanol demonstrates the microbial machinery and other factors required to produce methane from these substrates is present in the sediments from the investigated sites. The suggested implication is that mangrove ecosystems may be large methane emitters, provided the observations and model results accurately represent mangrove systems at large.

Although the diversity of data is limited, the authors do a commendable job of testing the hypothesis that non-competitive substrates accounted for the accumulation of methane in the sulfate reduction zone. The study does not provide definitive evidence that the process is active, as the only substrate-level data supporting its activity are from ex situ incubation experiments. The study should be used as motivation for tackling this specific question in greater detail in a mangrove ecosystem. It would appear others have observed the same effect in mangroves, but this appears to be the first to suggest a mechanism for the repeated observation. This is an important and interesting contribution. With moderate revisions, this reviewer recommends publication of this manuscript in Biogeosciences.

### Specific Comments:

1. The grouping of the profiles helps to consolidate the data in a way that makes the application of the model more systematic. However, the authors have a tendency to overstate the certainty of their findings. For example, the model does not “illustrate” that methane is produced from DOM...it suggests production from these unmeasured carbon sources is possible. Also, shallow methane production does not necessarily promote high methane fluxes to the water column and atmosphere as the authors state. Although benign in intent, these statements being expressed definitely in the abstract may be misleading because they imply the conclusions are based on data. Be clear that the conclusion are based on modeling results and that no measurements regarding fluxes were obtained.

Response:

We have changed the wording used to be more consistent with our data and less definitive (e.g. change "illustrate" to "suggests" and change "promote" to "increase the likelihood").

We have also made changes throughout the manuscript in order to more clearly differentiate the modeling results from the field and laboratory measurements.

This reviewer recommends the authors provide a figure with generalized sulfate profiles (and methane, if applicable) for each group in Fig 2. Such a model (and a description of each group in the Fig 2 headings) would give the reader a better intuitive sense for the groupings.

Response:

Fig. 2 was moved to supplementary material and replaced with a figure showing one of the typical profiles per group.

2. Why would mangroves have such a high abundance of non-competitive substrates in comparison to other brackish systems?

Response:

This is a question we can only speculate about. Mangrove forests are known to be highly productive ecosystems with the capacity to release high concentrations of DOM to sediment porewaters (Kristensen et al., 2008). Litter from trees (leaves, propagules and twigs) and subsurface root growth provide further significant inputs of organic carbon to mangrove sediments which are unique for this type of system. We have now included these sentences in the manuscript.

Kristensen, E., Bouillon, S., Dittmar, T., Marchand, C., 2008. Organic carbon dynamics in mangrove ecosystems: A review. *Aquatic Botany*, 89(2): 201-219.

3. Using the near surface methane gradients and modeled results, the authors should quantify the differing methane flux potentials for each environment rather than only speculating about the importance of this methane source.

Response:

Model derived methane fluxes to the water column are listed in Table 2 ( $F_{\text{methane (top)}}$ ) and reveal fluxes (0.011-21 mmol CH<sub>4</sub> m<sup>-2</sup>d<sup>-1</sup>) that are similar or up to two orders of magnitude larger than fluxes reported for other mangrove systems in Florida (0.02 mmol CH<sub>4</sub> m<sup>-2</sup>d<sup>-1</sup>, Barber et al., 1988; Harriss et al., 1988), Australia (0.03-0.52 mmol CH<sub>4</sub> m<sup>-2</sup>d<sup>-1</sup>, Kreuzwieser et al., 2003), and India (5.4-20.3 mmol CH<sub>4</sub> m<sup>-2</sup>d<sup>-1</sup>, Purvaja and Ramesh, 2001). Since all of the different types of methane depth profiles (Group-1, Group-2, etc) were found during each sampling trip and no differences in spatial and temporal distribution (seasons and sampling locations) were

observed, model derived methane effluxes to the water column and the variability in the porewater methane concentrations suggest a very dynamic system with high methane production and efflux rates. We have included this in the discussion section of the manuscript.

4. The site description should include a description of where and why anhydrite might contribute excess sulfate. An alternate possibility not discussed is oxidation of sulfides. Total sulfides were not measured, so their potential contribution cannot be discussed. Perry and others have written much about why anhydrites and gypsum are found on the Yucatan platform. More details would make this argument more convincing. The evidence for contributions from anhydrite are not especially compelling. Basically, the authors state that there is anhydrite in the area, so that explains the excess sulfate. From looking at one of the Perry references, it is not clear that one would expect a groundwater contribution in the Chelem lagoon (inside the Chicxulub impact zone). More details would be helpful. Sr data would be even better, but that is not likely to be available and is not required.

Response:

Perry et al. (2002) identified dissolution of evaporites within the freshwater lens as the probable source of the excess  $\text{SO}_4^{2-}$  found in some Yucatán groundwater by using the ratio between sulfate and chloride ( $100 \times (\text{SO}_4/\text{Cl})$ ). Ratios higher than seawater (average seawater is 10.3) are expected where gypsum/anhydrite dissolution is involved (Perry et al. 2002). The other indicator is Sr/Cl ratio which in groundwater is invariably higher than the seawater value and indicates dissolution of celestite (from evaporite) and/or aragonite (Perry et al. 2002). The region east and south of Lake Chichancanab, Mexico, referred to as the Evaporite Region by Perry et al. (2002) is characterized by distinctive topography and the high-sulfate content of groundwater (Perry et al. 2002). The groundwater from the presumed source region, Lake Chichancanab, flows northward into the Celestún Estuary which can be recognized by the progressive decrease in the ratio  $[\text{SO}_4/\text{Cl}]_{\text{groundwater}}/[\text{SO}_4/\text{Cl}]_{\text{seawater}}$  in water from southeast to northwest (Perry et al., 2009). These parameters in Celestún lagoon published in Young et al., (2008) are consistent with our interpretation that gypsum/anhydrite dissolution involved in the groundwater contribute to Celestún lagoon.

Though there are no published  $\text{SO}_4$  and Sr data for groundwater and surface water in Chelem lagoon, Perry et al., (2009) measured strontium concentrations greater than seawater in the saline groundwater of the Northern Yucatan Peninsula east of the Ring of Cenotes, and Chelem lagoon is located within this region. We included this in the discussion section of the manuscript.

5. Were the sediments dried and prepared for TOC analysis as part of this study, or Gonnee et al., 2004? The methods do not include the analysis. The results do not specify the origin of the data. Please clarify.

Response:

The original data are from Gonnee et al., (2004) and Eagle, (2002, master thesis). The TOC study utilized splits of the sediment cores collected for methane concentration analysis.

We have included both references in the manuscript.

6. Increasing OM content with depth? How is this? Suggestion of a changed depositional pattern not discussed.

Yes, organic matter profiles show a changed depositional pattern (Gonneea et al., 2004). Since this pattern can't be used for organic matter degradation calculations, we simulate  $[\text{SO}_4^{2-}]_{\text{dep}}$  profiles to derive organic matter degradation rates. To avoid the confusion between TOC analysis, TOC data expressions and reaction rates for  $R_{\text{organic}}$  (Eq. A11) and  $R_{\text{POC}}$  (Eq. A7) in this version, we have removed the sampling and analytical methods, results, discussions and the model equation related to the measured particulate organic contents from our manuscript and refer the measured organic matter contents to Gonneea et al (2004) and Eagle (2002, thesis).

7. Why would negative sulfate depletion be observed at the surface and not at depth if the source of the excess sulfate is from depth? See Core 7CH-Oct01.

Response:

It may be possible that some  $\text{H}_2\text{S}$  is oxidized in the shallow subsurface of the cores due to oxygen penetration due to bioturbation.

Therefore, excess sulfate could potentially be from  $\text{H}_2\text{S}$  oxidation and/or from sulfate input from groundwater. We note that in this specific site groundwater has been previously identified as a source of excess sulfate and excess Sr. We now include this option in the revised manuscript, whilst further noting that, since  $R_{\text{SD}}$  is the net sulfate depletion, model results may underestimate the true  $R_{\text{POC}}$  and  $R_{\text{M}}$  due to sulfide oxidation. However, this is only relevant for very few cores in Group-1 and Group-2 where a shallow subsurface excess sulfate is observed. Although we mention this option for completion we believe that groundwater input is a more likely source due to correlation between excess sulfate and excess Sr which has been previously described and is consistent with groundwater input.

Technical Corrections:

17921, line 21: 'porewater'

17923, line 7: delete 'that'

17923, line 12: 'sites'

17927, line 5: 'inhibited'

17930, line 3: 'atmosphere'

17920, line 20: 'chloride'

Response:

These technical corrections have been revised in the manuscript.

Figures:

1. Put letters on the figure panels

Response:

The figure has been revised.

2. Some units on figures indecipherable (e.g., CH<sub>4</sub> conc)

Response:

The figure has been revised.

## **A list of all relevant changes made in the manuscript:**

Dear editor,

Based on both referees' comments, we have incorporated our responses in the revised manuscript. The relevant changes are as follows:

1. modifying model descriptions which include AOM and heterotrophic sulfate reduction ( $R_{SR}$ ) into net sulfate depletion rates ( $R_{SD}$ ), use  $R_{SR}=R_{SD}$  and use 5 yrs for steady state simulations;
2. combining cores for Group-2 and Group-3 into one group, so there are four Groups of porewater profiles;
3. using the second modeling approach to simulate the original Group-2 data which has been combined with Group-3 in this version;
4. adding methanogenesis rates calculated from sediment slurry experiments in Table 1, adding maximum model-derived rates of methanogenesis and sulfate reduction in Table 3 and comparing both methanogenesis rates in the main text;
5. removing the sampling and analytical methods, results, discussions and the model equation related to the measured particulate organic contents from our manuscript and refer the measured organic matter contents to Gonnee et al (2004) and Eagle (2002), since organic matter profiles show a changed depositional pattern which can't be used for organic matter degradation calculations;
6. adding the sampling and analytical methods and results for porewater methane;
7. including a description of where and why anhydrite might contribute excess sulfate in the discussion section of the manuscript, though oxidation of sulfides is a possible source for excess sulfate;
8. including model derived methane fluxes to the water column listed in Table 2 ( $F_{methane(top)}$ ) in the discussion section of the revised manuscript;
9. including additional discussion to show there is no relation between profile time and location or season and that the variability is a result of the system being heterogeneous and probably highly dynamic;
10. describing AOM plays a minor role in this study in the last paragraph;
11. showing one selected profile per group in Fig. 2 for illustration and presenting the other profiles for each group (9 cores for Group-1, 6 cores for Group-2, 2 cores for Group-3 and 3 cores for Group-4) in the Appendix (Fig. A1);
12. revising all Tables according to modified modeling approaches (there are no mark-up changes for Tables shown in this file);
13. improving English structures and presentations;
14. improving qualities of all figures.
15. Andrew Dale (GEOMAR) has been added as a co-author for his contribution and advice on the numerical modelling.

1 **Methane and Sulfate Dynamics in Sediments from Mangrove-dominated**  
2 **Tropical Coastal Lagoons, Yucatán, Mexico**

3  
4 **P.-C. Chuang<sup>1</sup>, M. B. Young<sup>2</sup>, A. W. Dale<sup>3</sup>, L. G. Miller<sup>2</sup>, J. A. Herrera-Silveira<sup>4</sup>, A.**  
5 **Paytan<sup>1,5</sup>**

Deleted: 3

Deleted: 4

6  
7 [1] Department of Earth and Planetary Sciences, University of California Santa Cruz, 1156  
8 High St., Santa Cruz, CA 95064, United States

9 [2] U.S. Geological Survey, 345 Middlefield Rd, MS 434, Menlo Park, CA 94025, United  
10 States

11 [3] GEOMAR Helmholtz Centre for Ocean Research Kiel, Wischhofstr. 1–3, 24148 Kiel,  
12 Germany

13 [4] CINVESTAV-IPN, Unidad Mérida, A.P. 73 CORDEMEX, Mérida, Yucatán, Mexico

Deleted: 3

14 [5] Institute of Marine Sciences, University of California Santa Cruz, 1156 High St., Santa  
15 Cruz, CA 95064, United States

Deleted: 4

16  
17 Correspondence to: P.-C. Chuang ([pchuan2@ucsc.edu](mailto:pchuan2@ucsc.edu); [pcchuang2@gmail.com](mailto:pcchuang2@gmail.com))

1 **Abstract**

2 Porewater profiles in sediment cores from mangrove-dominated coastal lagoons (Celestún and  
3 Chelem) on the Yucatán Peninsula, Mexico, reveal the widespread coexistence of dissolved  
4 methane and sulfate. A numerical transport-reaction model suggests that methane in the upper  
5 sediments is produced in the sulfate reduction zone at rates ranging between 0.012 and 31  
6 mmol m<sup>-2</sup> d<sup>-1</sup>, concurrent with sulfate reduction rates between 1.1 and 24 mmol SO<sub>4</sub><sup>2-</sup> m<sup>-2</sup> d<sup>-1</sup>.  
7 The model also indicates that a significant fraction of methane is transported to the sulfate  
8 reduction zone from deeper zones within the sedimentary column, by rising bubbles and gas  
9 dissolution. Sediment slurry incubation experiments show that non-competitive substrates such  
10 as trimethylamine (TMA) and methanol can be utilized for microbial methanogenesis at the  
11 study sites. Our results suggest that a large fraction of the methane formed in the sediments  
12 escapes to the overlying water column. By combining field measurements with  
13 transport-reaction modeling, we are able to demonstrate that sediments in coastal lagoons  
14 within mangrove ecosystems are characterized by shallow methane production and  
15 accumulation depths, likely due to non-competitive substrate utilization in near-surface  
16 sediments and extensive bubble transport and dissolution; this may favor high methane  
17 emission rates.

19 **1 Introduction**

20 Wetlands are the largest natural source of methane (CH<sub>4</sub>) to the atmosphere, accounting for  
21 between 20-25% of the global atmospheric methane budget (Fung et al., 1991; Whalen 2005).  
22 Methane produced in wetlands is primarily biogenic, arising from microbial activity in  
23 anaerobic sediments and soil. Since sulfate-reducing bacteria outcompete methanogens for  
24 common substrates (Oremland and Polcin, 1982), freshwater wetlands typically have much  
25 higher methane fluxes to the atmosphere than brackish to fully marine wetlands (Bartlett et al.,  
26 1987; Bartlett et al., 1985; Segarra et al., 2013). Marine and estuarine sediments are generally  
27 characterized by comparatively lower rates of methanogenesis with a methane production and  
28 accumulation zone located deeper within the sediment pile below the sulfate reduction zone,  
29 (Holmer and Kristensen 1994; Martens and Val Klump 1984; Poulton et al., 2005; Segarra et  
30 al., 2013). In these marine or estuarine systems methane that diffuses upwards towards the  
31 sediment surface can be oxidized both anaerobically (AOM) and aerobically within the  
32 sediments and in the water column, reducing emissions to the atmosphere (Whalen, 2005).  
33 Despite brackish to marine salinities, methane fluxes comparable to those measured in  
34 freshwater wetlands have been reported for coastal mangrove-dominated lagoon systems in

- Deleted:** due to
- Deleted:** Methane, sulfate and chloride concentrations in sediment porewater from two coastal mangrove ecosystems (Celestún and Chelem Lagoons) on the Yucatán Peninsula, Mexico were measured. In these sediments methane exists in shallow sediments where sulfate is not depleted, and sulfate reduction is actively occurring. A transport-reaction model depicting the various production and consumption processes for methane and sulfate is used to elucidate processes responsible for this observation. The model illustrates that methane in the upper sediments is produced in-situ supported by high dissolved organic matter as well as by non-competitive substrates. In addition methane is contributed to porewater in the upper sediments, where sulfate reduction occurs, by transport from deeper zones within the sedimentary column through bubbles dissolution and diffusion. The shallow methane production and accumulation depths in these sediments promote high methane fluxes to the water column and atmosphere.
- Deleted:** The primary source of this methane is microbial activity within anaerobic wetland sediments.
- Deleted:** Freshwater
- Deleted:** atmospheric
- Deleted:** to saline coastal areas
- Deleted:** ,
- Deleted:** due primarily to the ability of sulfate-reducers to outcompete methanogens for shared substrates. Therefore saline and brackish sediments are
- Deleted:** either
- Deleted:** , deeper zones of methanogenesis, or both
- Deleted:** Methane can be oxidized both aerobically and anaerobically within the sediments and water column, reducing emission to the atmosphere
- Deleted:** The depth at which methanogenesis occurs will determine the time of exposure to potential oxidizing conditions within the sediments, and can have a large effect on how much of the total methane produced is released from the sediments to the water column and atmosphere.
- Deleted:** high
- Deleted:** ,
- Deleted:** ,
- Deleted:** eco

1 several places around the world, including Florida (Barber et al., 1988), Puerto Rico  
2 (Sotomayor et al., 1994), India (Biswas et al., 2004; Biswas et al., 2007; Purvaja and Ramesh,  
3 2000; Purvaja and Ramesh, 2001; Ramesh et al., 1997; Ramesh et al., 2007; Verma et al.,  
4 1999), Tanzania (Kristensen et al., 2008), Thailand (Lekphet et al., 2005), China (Alongi et al.,  
5 2005), Andaman Islands (Linto et al., 2014) and Australia (Call et al., 2015). The anaerobic  
6 and organic-rich sediments found in these systems provide a suitable environment for  
7 methanogenesis, yet the extensive supply of sulfate from seawater should favor sulfate  
8 reducers over methanogens in the shallow sections of the sediments (Kristensen et al., 2008;  
9 Lee et al., 2008). There are, however, several possible ways for coastal mangrove lagoons to  
10 sustain relatively high methane fluxes despite high sulfate concentrations. For example, if the  
11 microbial activity of sulfate reducers is high and sulfate replenishment from the overlying  
12 water is slow, sulfate may become depleted in the upper centimeters of the sediment, thus  
13 allowing methanogens to occur close to the sediment surface. Additionally, methanogens can  
14 co-exist with sulfate reducers when non-competitive substrates (those used only by  
15 methanogens and not by sulfate reducers) are available. Moreover, in these systems methane  
16 may migrate from deeper in the sediment to shallower depth and to the water column.  
17 Typically, a large percentage of the methane produced in sediments is oxidized prior to  
18 reaching the atmosphere, and in shallow-water systems, the oxidation takes place primarily in  
19 the sediments and not in the water column (Martens and Valklump 1980; Mitsch and Gosselink,  
20 2000; Weston et al., 2011; Segarra et al., 2013, 2015). However, accumulation and transport of  
21 methane in gas bubbles reduces the exposure time of methane to oxidants such as oxygen and  
22 sulfate, allowing a large fraction of gas to escape the sediment (Barnes et al., 2006; Martens  
23 and Valklump, 1980).

24 The objective of this study was to examine porewater methane distribution within the  
25 sediments of two mangrove-dominated coastal lagoons in Mexico and relate them to sulfate  
26 concentrations of the sediments. We aim to gain a better understanding of the factors  
27 controlling the methane flux from coastal mangrove-dominated lagoon sediments. To this end,  
28 we applied a numerical transport-reaction model based on Wallmann et al. (2006) and Chuang  
29 et al. (2013) to simulate porewater methane and sulfate concentration profiles. We also  
30 performed sediment slurry incubation experiments to test the effect of competitive and  
31 non-competitive substrates on methanogenesis in the lagoon sediments. The results provide  
32 quantitative data on methane dynamics in coastal mangrove-dominated lagoon systems and  
33 highlight their importance as methane sources to the atmosphere.

## 34 2 Study sites

Deleted: .  
Deleted: .  
Deleted: and the Yucatán Peninsula (Chuang et al., 2015).  
Deleted: mangrove eco

Deleted: that  
Deleted: wetland sediments can  
Deleted: I  
Deleted:  
Deleted: very  
Deleted: rapidly  
Deleted: few  
Deleted: dominate just below this zone  
Deleted: within the sediment

Deleted: The mechanism of gas release from the sediment can also affect exposure time to oxidizing conditions in the sediment and may therefore have a significant effect on the total methane flux to the atmosphere.  
Deleted: A

Deleted: If enough methane builds up within the sediment, it can be released in the form of bubbles (ebullition), which can travel through the sediment and water column quickly, resulting in minimal oxidation

Deleted: purpose

Deleted: in order to better understand the processes controlling methane flux from these sediments to the water column and atmosphere in these systems. By examining the spatial and temporal differences in porewater methane distributions at the mangrove lagoons, and relating them to sulfate concentrations and organic carbon content of the sediments, we can gain a better understanding of the factors controlling atmospheric methane flux from coastal mangrove ecosystems.

Deleted: do this

Deleted:

Deleted: the

Deleted: used

Deleted: in

Deleted: in order to understand factors controlling sources and sinks of porewater sulfate and methane and to assess rates of biogeochemical reactions in this dynamic system.

Deleted: .

Deleted: area

1 Fieldwork was conducted in two mangrove-dominated coastal lagoons located on the western  
2 Yucatán Peninsula, Mexico (Figure 1). The typical climatological pattern for this area consists  
3 of a dry season (March–May), a rainy season (June–October) during which the majority of the  
4 annual rainfall (>500mm) occurs, and the “nortes” season (November–February), which is  
5 characterized by moderate rainfall (20-60mm) and intermittent high wind speeds greater than  
6 80 km hr<sup>-1</sup> (Herrera-Silveira, 1994).

Deleted: Sampling for this study

7 Celestún Lagoon (20°52'N, 90°22'W) is long, narrow, and relatively shallow (average depth =  
8 1.2 m). The inner and middle sections of the lagoon always have lower salinities than the  
9 section near the mouth due to year-round discharge of brackish groundwater from multiple  
10 submarine springs (Young et al., 2008). Salinity within the lagoon fluctuates seasonally, with  
11 salinity in the inner zone ranging from 8.9 to 18.2 during the course of this study, grading out  
12 to marine salinities at the mouth of the lagoon (Young et al., 2008). The lagoon is surrounded  
13 by 22.3 km<sup>2</sup> of well-developed mangrove forest, and has experienced relatively little  
14 disturbance from human development and/or pollution such as wastewater discharge  
15 (Herrera-Silveira et al., 1998). Sediments in Celestún consist primarily of autochthonous  
16 carbonate ooze.

Deleted: ... [1]

17 Chelem Lagoon (21°15'N, 89°45'W) (average depth = 0.7 m), in contrast, receives very little  
18 groundwater input and the surrounding area has been heavily impacted by urban development.  
19 Salinity in Chelem ranges from brackish to hypersaline (24.8 - 40.3 during the study period),  
20 and vegetation surrounding the lagoon consists of scrub mangrove forest (Young et al., 2008).  
21 The construction of Yucalpeten Harbor in 1969 (Valdes and Real 1998) increased the  
22 circulation and resulted in sandy marine sediments entering the lagoon. Sediments in Chelem  
23 deposited since 1969 consist of a heavily bioturbated mix of sands and autochthonous  
24 carbonate ooze, with a large number of shells of living and dead burrowing organisms (Valdes  
25 and Real 1998). In the following text, CEL and CH denote cores collected from Celestún  
26 Lagoon and Chelem Lagoon, respectively.

Deleted: area

Deleted: the lagoon

Deleted: within the lagoon,

27

Deleted: -

### 28 3 Sampling and analytical methods

#### 29 3.1 Porewater solutes

Deleted: and organic carbon content

30 Sediment cores were collected along lengthwise transects in both lagoons during the three  
31 different seasons: April 2000 (dry season), December 2000 (nortes season), and October 2001  
32 (late rainy season). Duplicate samples (1\_1CH\_Oct01 and 1\_2CH\_Oct01) were collected at  
33 station 1CH in Chelem lagoon. Sediments were sampled using hand-held acrylic push cores (7  
34 cm inner diameter) either 30 or 60 cm in length. The push cores had holes drilled along the side

Deleted: . Sampling was conducted in Celestún and Chelem in

Deleted: -

1 at 2 cm intervals, which were sealed with electrical tape prior to sampling. Subsamples for  
2 porewater methane analysis were collected in the field immediately after core collection from  
3 the holes along the sides of the push cores, using plastic 3 mL syringes with the needle  
4 attachment end removed. The sediment plugs from the syringes were immediately extruded  
5 into 20 mL glass Wheaton bottles and sealed with blue butyl stoppers and aluminum crimp  
6 caps. 3 mL of degassed Milli-Q water and 0.3 mL of saturated mercuric chloride (HgCl<sub>2</sub>)  
7 solution were added to create a slurry and halt all biological activity within the sample.

Deleted: [CH<sub>4</sub>]

8 After subsampling, the cores were capped, the holes were resealed, and the cores were  
9 transported back to the lab for sectioning and porewater extraction. The cores were extruded  
10 and sliced into 2.5 cm depth intervals in an anaerobic glove bag under an N<sub>2</sub> atmosphere and  
11 transferred into centrifuge tubes for porewater extraction. Core length was measured  
12 immediately after collection and just prior to extrusion in order to correct for compaction  
13 during transport. Average compaction was 6% of the total core length, and never exceeded  
14 20%.

Deleted: sediment

Deleted: and methane concentrations were measured as described in (Chuang et al., 2015).

Deleted: In the laboratory, t

Deleted: , then

15 Porewater for sulfate (SO<sub>4</sub><sup>2-</sup>) and chloride (Cl<sup>-</sup>) analysis was extracted by centrifuging all the  
16 sediment from each depth interval and filtering the porewater through sterile 0.20 μm syringe  
17 filters. Samples were kept frozen in 20 mL acid-cleaned glass scintillation vials until analysis.

Deleted: -

Deleted:

18 Porewater sulfate and chloride concentrations were measured by ion chromatography using a  
19 Dionex DX-500 IC equipped with an Ionpac AS9-HC column (4mm) and AG9-HC (4mm)  
20 guard column. The samples were diluted 5-fold with Milli-Q water prior to analysis in order to  
21 bring the sulfate and chloride within the appropriate analytical range for the ion  
22 chromatograph.

Deleted: to separate

Deleted: from the sediment, then passing the porewater

Deleted: inside an anaerobic chamber. Porewater s

Deleted: and stored frozen

Deleted: -

Deleted: [SO<sub>4</sub><sup>2-</sup>]

Deleted: [Cl<sup>-</sup>]

Deleted: [SO<sub>4</sub><sup>2-</sup>]

Deleted: [Cl<sup>-</sup>]

Deleted: After porewater extraction, sediment samples were dried and prepared for analysis of organic carbon content (C<sub>organic</sub>) as described in (Gonneea et al. 2004).

23 Methane concentrations for all samples were measured on an SRI 310 Gas Chromatograph  
24 (GC) equipped with a flame ionization detector and an Alltech Haysep S 100/120 column (6' x  
25 1/8" x 0.085"). Helium was used as the carrier gas at a flow rate of 15 ml/min and the column  
26 and detector temperatures were maintained at 50 °C and 150 °C, respectively. Peak integration  
27 was performed using Peak Simple NT software. Methane gas standards were prepared by  
28 diluting 100% methane in helium, and five standards bracketing the range of sample  
29 concentrations were measured at the beginning, middle, and end of each set of analyses.  
30 Average standard error of repeat injections of standards throughout a sample run (between 2 to  
31 6 hours of continuous analysis) was 1.8% (n=152). Porewater methane concentration in the  
32 sediment core subsamples was determined after vigorously shaking of the sealed serum bottles  
33 containing the sediment slurries to ensure complete mixing, followed by at least 3 minutes of  
34 standing equilibration time to ensure that the porewater methane was fully equilibrated with the

1 headspace in the serum bottles. A small volume of headspace (0.25-0.5  $\mu$ L) was drawn out of  
2 each serum bottle using a gas-tight syringe, and analyzed for methane concentration on the SRI  
3 310 GC. The total volume of porewater in each sample was calculated using the difference  
4 between the total wet weight of the sediment minus the dry weight of the sediment, correcting  
5 for the added water and HgCl<sub>2</sub> solution.

Deleted: -

### 7 **3.2 Sediment slurry incubation experiments**

8 Sediment slurry incubations were performed in order to examine changes in methane  
9 production over different time intervals and at different substrate concentrations (Table 1).

10 Incubations consisted of three competitive substrates (H<sub>2</sub>, acetate, formate), two  
11 non-competitive substrates (methanol, trimethylamine (TMA)), and four types of controls. The  
12 controls (preparation methods are described below) consisted of an un-amended sediment  
13 control under anaerobic conditions, an un-amended aerobic control (partial oxygen headspace),  
14 a killed control in which the sediment was autoclaved to kill all living organisms in the  
15 sediment, and a chemical control in which biological methanogenesis was inhibited through the  
16 addition of 2-bromoethanesulfonic acid (BES) to a final concentration of 40 mM within the  
17 slurry. Triplicate bottles were prepared for each condition (controls and substrate additions),  
18 and methane headspace concentrations were measured at 3-4 time intervals over the course of  
19 29 days.

Deleted: 3

Deleted: 2

Deleted: 4

Deleted: m

Deleted: m

20 All the sediment slurries were prepared semi-anaerobically by homogenizing sediment in a  
21 blender with artificial seawater mixture in a 1:1 ratio under continuous flow of nitrogen gas.  
22 Large pieces of leaves, twigs, and shells were removed from the sediment prior to  
23 homogenization. 70 mL glass Wheaton bottles were flushed with nitrogen gas for 1 minute  
24 prior to the addition of the sediment slurry. 30 mL of slurry was then added to each bottle under  
25 continuous nitrogen flow, and the bottles were sealed using blue butyl rubber stoppers and  
26 aluminum crimp seals. Substrate additions were made by injecting the substrate solution into  
27 the bottle immediately after sealing the bottles, except for the H<sub>2</sub> gas treatment and the aerobic  
28 control. For the addition of H<sub>2</sub>, the entire headspace of the bottles was flushed with 100% H<sub>2</sub>  
29 gas. After each headspace sampling the H<sub>2</sub> gas removed by microbial activity in the sediment  
30 was replaced by inserting a gas tight syringe filled with 100% H<sub>2</sub> gas into the bottles, and  
31 allowing the gas to be drawn into the bottles until equilibrium pressure was reached. The  
32 aerobic controls were prepared like the anaerobic un-amended controls, except that 8 mL (20%  
33 of the total headspace) of 100% O<sub>2</sub> was added to the bottles immediately after they were sealed.  
34 In order to ensure that the sediment slurries remained aerobic, 100% O<sub>2</sub> was added to the  
35 bottles throughout the incubation period. The sediment slurries were kept at room temperate

Deleted: ,

Deleted: no

Deleted: amendment

1 (22°C) and agitated continuously on a shaker table throughout the course of the incubations.  
2 Headspace samples (0.25 mL) were extracted from the bottles at each time interval using a  
3 gas-tight syringe. Methane concentrations were measured on an HP 5730A GC equipped with a  
4 flame ionization detector. GC calibration and creation of standard curves were based on  
5 successive dilutions of 100% methane. Analytical error was approximately 5% for methane  
6 concentrations below 10 ppm-v (446 nM), and less than 3% for methane concentrations above  
7 10 ppm-v as determined by repeat analyses of standards and samples.

Deleted: gas chromatograph (

Deleted: )

Deleted: CH<sub>4</sub>

Deleted: CH<sub>4</sub>

Deleted: CH<sub>4</sub>

## 8

### 9 4 Results

#### 10 4.1 Porewater concentrations of dissolved species

11 Representative porewater methane profiles were plotted alongside sulfate profiles in Fig. 2, and  
12 Fig. A1. Profiles were assigned to one of four profile-types based on the relation between  
13 methane and sulfate distributions down core (see below). Considerable spatial and temporal  
14 variability in porewater chemistry was observed with no systematic seasonal differences in  
15 concentration trends. For example, porewater methane concentrations varied by up to three  
16 orders of magnitude in both lagoons, even between sites in close proximity to each other (i.e.  
17 ICEL and 2CEL, Oct01; 1CH and 2CH, Dec00), and at the same station sampled during  
18 different seasons (i.e. 2CEL Dec00, Oct01; 1CH Apr00 and Oct01). No consistent differences  
19 were evident between the stations at the sides of the lagoons and those located in the center of  
20 the lagoons, or between stations located in the inner zone of the lagoons and those located near  
21 the mouth. For instance, methane above calculated saturated concentrations (1.1 and 1.3 mM)  
22 was observed in cores ICEL Jul02 (the inner zone of Celestún lagoon) and 14CEL Dec00  
23 (near the mouth of Celestún lagoon). This is particularly interesting because the mouth of the  
24 lagoon has much higher salinities than the inner zone (Young et al., 2008). The variability (both  
25 spatial and temporal) in the porewater methane concentrations and in the spatial and temporal  
26 distribution of profile types suggest a very dynamic system where both concentration and  
27 distribution patterns in the porewater vary constantly (spatially throughout the lagoons and  
28 temporally at distinct sites). Such variability is indicative of rapid methane production and  
29 efflux rates.

Deleted: reported in Chuang et al., (2015) are plotted alongside sulfate profiles

30 Porewater sulfate concentrations ranged from 0.21 to 35.3 mM in Celestún lagoon and from  
31 4.13 mM to 33.5 mM in Chelem lagoon and show different trends (Fig. 2; Fig. A1). In many of  
32 the cores a negative relation between methane and sulfate was observed. Specifically, higher  
33 sulfate was associated with lower methane in cores located near the mouth of the lagoons  
34 (16CEL Jul02, 16CEL Oct01, 14CEL Oct01, 14CEL Jul02 and 5CH Apr00) and lower

Deleted: Duplicate samples (1\_1CH\_Oct01 and 1\_2CH\_Oct01) were collected at station 1CH in Chelem lagoon.

Deleted: mM

Deleted: is

Deleted: particularly

1 sulfate with high methane in the inner zone of the lagoons (e.g. cores ICEL\_Jul02,  
2 ICEL\_Dec00, 3CEL\_Jul02, 3CEL\_Apr00, 1\_1CH\_Oct01, and 1\_2 CH\_Oct01).

3 The relationship between porewater salinity (represented by chloride concentration), methane  
4 and sulfate concentrations was spatially and temporally variable (Fig. 3). Generally, higher  
5 sulfate concentrations were associated with higher chloride in cores located near the mouth of  
6 the lagoons and lower sulfate with lower chloride in the inner zone of the lagoons (Fig. 3A).  
7 Despite these general trends there are no clear consistent relationships between methane and  
8 chloride (Fig. 3B) and sulfate and methane (Fig. 3C) when the data was considered collectively.  
9 The lack of consistent trends suggests multiple processes impacting the distribution of methane  
10 and sulfate. These include physical processes, such as mixing and dilution with seawater or  
11 groundwater, and biological processes such as sulfate reduction, methanogenesis and methane  
12 oxidation. Brackish groundwater enters the Celestún lagoon through at least 30 subsurface  
13 discharge points (Young et al., 2008), and the chloride profiles suggest that some of this  
14 groundwater may seep through the sediments, resulting in localized decline in porewater  
15 salinities.

16 To account for mixing with seawater or freshwater and to extract information on the processes  
17 controlling the distribution of porewater solutes, the observed sulfate depletion ( $[SO_4^{2-}]_{dep}^{OBS}$ )  
18 relative to seawater was calculated as the difference between the expected sulfate concentration  
19 contributed from seawater (based on porewater chloride concentration) and the measured  
20 sulfate concentration:

$$[SO_4^{2-}]_{dep}^{OBS} = \frac{[SO_4^{2-}]_{(sw)}}{[Cl^-]_{(sw)}} \times [Cl^-]_{(measured)} - [SO_4^{2-}]_{(measured)} \quad (1)$$

24 where 0.05171 is applied for the  $\frac{[SO_4^{2-}]_{(sw)}}{[Cl^-]_{(sw)}}$  ratio (Pilson, 1998). Positive values indicate that  
25 sulfate has been removed from the porewater, most likely through sulfate reduction while  
26 negative values indicate an external source of sulfate not associated with chlorine that is other  
27 than seawater, in this case the groundwater (see discussion below).

28 Based on the observed trends in sulfate depletion, when considered together with methane, four  
29 different porewater trends can be described, referred to as Groups 1 through 4 here (Fig. 2, Fig.  
30 A1). The majority of profiles fell into Group-1 (10 cores); these profiles showed positive  
31 sulfate depletion profiles (e.g. sulfate consumption or loss) with methane profiles mirroring the  
32 sulfate concentration profiles (methane production or input). The peaks for methane and sulfate  
33 depletion occurred at the same depth as the lowest measured sulfate concentrations. In Group-2

Deleted: porewater [CH<sub>4</sub>], and porewater [SO<sub>4</sub><sup>2-</sup>] appears to be

Deleted: Fig. 2;

Deleted: H

Deleted: is

Deleted: all

Deleted: is

Deleted: together

Deleted: between chlorine (salinity), sulfate and methane in the cores

Deleted: these parameters

Deleted: ,

Deleted: ing

Deleted: that are not sensitive to salinity

Deleted: production and

Deleted: Specifically, b

Deleted: and enable deciphering the physical and biological

Deleted: ere

Deleted: determined

Deleted: analysis

Deleted: .

Deleted: 0

Deleted: fall into five

Deleted: In Group-1,

Deleted: show positive values

Deleted: ,

Deleted: and sulfate

Deleted: are at the same depth

1 (7 cores), sulfate depletion sulfate depletion also showed positive values (sulfate consumption)  
 2 but not throughout the core. In some cores sulfate depletion was close to zero at shallow depths  
 3 and then increased with depth and in other cores positive sulfate depletion values appeared at  
 4 the surface of the sediments and then decreased to almost zero at deeper depths. Methane  
 5 concentrations for this group showed no clear relation to the sulfate profiles. In Group-3 (3  
 6 cores), sulfate depletion showed negative values (e.g. sulfate addition). The values became  
 7 more negative toward the deeper sediment starting from zero right at the surface suggesting  
 8 that sulfate was being added from the bottom of the sediment section. In Group-4 (4cores),  
 9 there was almost no sulfate depletion (sulfate concentrations similar to seawater) from the  
 10 surface to the deeper depths and methane concentrations were low (< 0.25 mM) increasing at  
 11 depth, indicating a deeper source of methane.

13 **4.2 Sediment slurry incubation experiments**

14 All the sediment slurries with added substrates showed an increase in headspace methane  
 15 concentrations that was significantly greater than those observed with either the un-amended  
 16 aerobic and anaerobic controls or the treated controls (Figure 4). The greatest increases in  
 17 headspace methane concentration were seen with additions of the two noncompetitive  
 18 substrates, TMA and methanol. The H<sub>2</sub> treatment showed the next highest methane production  
 19 rate, followed by formate then acetate. Of the four control conditions, the un-amended  
 20 anaerobic treatment had the highest increase in headspace methane concentration than the  
 21 un-amended, anaerobic treatment, although there was no detectable change in the headspace  
 22 methane concentration in the aerobic treatment between 150 and 700 hours. Both the  
 23 autoclaved and BES treatments did not show any changes in headspace methane concentration  
 24 greater than the instrumental detection limits. The maximum methane production rates for each  
 25 treatment are listed in Table 1.

27 **5 Discussions**

28 **5.1 Co-existence of Methane and Sulfate in Sediments**

29 Seawater transport into the sediment by diffusion and bioirrigation due to the activity of  
 30 burrowing animals has clear effects on porewater solutes. These processes are a source of  
 31 seawater sulfate and mask sulfate loss by microbial reduction. Although, as indicated above,  
 32 considerable variability in porewater profile distribution trends was observed, and different  
 33 profile types were found throughout the lagoons, certain trends were more common at distinct  
 34 locations. Specifically, sites characterized by sulfate addition from input of seawater into the

**Deleted:** is close to zero at surface depths and then increase with increasing depth which indicate sulfate input from the overlying water column and sulfate consumptions at depth. Methane concentrations for this group are scattered showing no relation to sulfate profiles.

**Deleted:** positive

**Deleted:** appear at the surface sediments and then decrease to almost zero at deeper depths. Methane profiles do not show strong relations with respect to sulfate depletion profiles in this group

**Deleted:** the trend for sulfate depletion is similar to that of Group-3 with decreasing values toward the deeper sediment but starting from zero right at the surface. The negative sulfate depletion values and porwater sulfate concentrations above seawater values (>28 mM) imply extra sulfate input from deeper depths. In Group-5,

**Deleted:** is

**Deleted:** are

**Deleted:**

**Deleted:** from surface to deeper depths

**Deleted: Organic matter content** ... [2]

**Deleted:** s

**Deleted:** methane

**Deleted:** seen

**Deleted:** no a

**Deleted:** ment

**Deleted:** 5

**Deleted:** [CH<sub>4</sub>]

**Deleted:** CH<sub>4</sub>

**Deleted:** no

**Deleted:** ment

**Deleted:** overall

**Deleted:** [CH<sub>4</sub>]

**Deleted:** The aerobic treatment had an initial higher increase in headspace [CH<sub>4</sub>] than the no amendment, anaerobic treatment

**Deleted:** [CH<sub>4</sub>]

**Deleted:** [CH<sub>4</sub>]

**Deleted:**

**Deleted:** .

**Deleted:** This results in addition of

**Deleted:** from the seawatermixing through diffusion and irrigation into the sediment has clear effects on porewater solutes. Specifically the mixing results in dilution of the methane in the porewater and enrichment of sulfate from seawater, hence

**Deleted:** ing

**Deleted:** any

**Deleted:** depletion values (e.g. rates of sulfate replenishments surpass sulfate reduction rates)

**Deleted:** While

**Deleted:** seen

1 sediment (cores in Group-4) were found primarily near the mouth of both lagoons where low  
2 methane was associated with near-zero sulfate depletion. Negative sulfate depletion (Group-3),  
3 on the other hand, which indicates the presence of porewater that is enriched in sulfate relative  
4 to chlorine, was seen primarily in the middle zone of Celestún Lagoon where groundwater  
5 springs rich in sulfate due to anhydrite dissolution are present, as reported by Perry et al. (2009;  
6 2002). Positive sulfate depletion profiles co-occurring with methane (Groups 1 and 2) were  
7 seen throughout the lagoons but mostly at sites in the inner zone of both lagoons, suggesting  
8 significant sulfate reduction at rates higher than the replenishment from sulfate rich  
9 groundwater or from the overlying seawater and a source of methane to the shallow sections of  
10 the sediment.

11 It is surprising that at many sites particularly within Groups 1 and 2 in the inner zone of both  
12 lagoons (ICEL, 2CEL, 3CEL and 1CH) high concentrations of methane and sulfate  
13 co-occurred at the same depth in the sediment. Co-existence of methanogenesis and sulfate  
14 reduction is not normally observed because sulfate reduction is more energetically favorable  
15 than methanogenesis, and sulfate reducers should outcompete methanogens for common  
16 substrates such as hydrogen and acetate (Oremland and Polcin, 1982; Jørgensen and Kasten,  
17 2006). Moreover, anaerobic oxidation of methane (AOM) coupled with sulfate reduction at the  
18 base of the sulfate reducing zone should further deplete methane (Capone and Kiene, 1988;  
19 Valentine and Reeburgh, 2000). There are several possible explanations for these observations.  
20 First, the high methane concentrations measured in the sulfate rich porewater may be supplied  
21 by a rapid non-diffusive mechanism from below the sulfate reduction zone (like rising gas  
22 bubbles), limiting the exposure time to AOM. Second, methane may be produced *in-situ* at  
23 these depths supported by a high abundance of competitive substrates in the sulfate reduction  
24 zone hence sustaining both methanogenesis and sulfate reduction (Holmer and Kristensen,  
25 1994). Third, methanogens may instead be able to thrive on various non-competitive substrates  
26 (Oremland and Polcin, 1982; Wellsbury and Parkes, 2000; Lee et al., 2008; Taketani et al.,  
27 2010). Indeed, use of non-competitive substrates by methanogens, including methanol,  
28 trimethylamines and dimethylsulfide, has been reported for mangrove sediments, coastal  
29 lagoons and continental shelf sediments (Ferdelman et al., 1997; Lyimo et al., 2000; Mohanraju  
30 et al., 1997; Purvaja and Ramesh, 2001; Torres-Alvarado et al., 2013; Maltby et al., 2016). Our  
31 slurry incubation experiments demonstrated that the methanogenic community at Celestún is  
32 capable of using a wide range of substrates, including H<sub>2</sub>, acetate, formate, methanol, and  
33 trimethylamine (Fig. 4). Both methanol and trimethylamine are not utilized by sulfate reducers,  
34 which could allow methanogens to thrive in the sulfate reduction zone (Fig. 4). The use of  
35 non-competitive substrates by the methanogenic community has important implications for

**Deleted:** This process is best seen near the mouth of the lagoon where low methane is associated with close to zero sulfate depletion. Negative sulfate depletion indicates mixing with water that is rich in sulfate relative to seawater and does not carry significant amounts of methane. Such conditions are seen primarily in the middle zone of Celestún Lagoon where groundwater springs input that is rich in sulfatedue to anhydrite dissolution in the aquifer has been recorded . Positive sulfate depletion profiles occur at sites located in the inner zone of the lagoon suggesting significant sulfate reduction at rates higher than any replenishment from sulfate rich groundwater or seawater. -

**Deleted:** some

**Deleted:**

methane fluxes to the atmosphere as it allows for methane production at shallow depths in the sediment and reduces the potential for complete oxidation of methane. Although processes and trends similar to those described above have been reported for other mangrove sediments (e.g., Lee et al., 2008; Purvaja and Ramesh, 2001), the co-occurrence of sulfate and methane and related biogeochemical reactions in these reports remain qualitative in nature. In the following section, we use a transport-reaction model to better quantify the processes controlling methane fluxes from the sediments in these mangrove-dominated tropical coastal lagoons.

## 5.2 Model set-up and application to mangrove-dominated coastal lagoon sediments

In order to understand methane production and consumption and how these processes relate to sulfate dynamics in the lagoon sediments, we used two different approaches to simulate methane and sulfate porewater profiles.

In the first approach, a transport-reaction model was applied to profiles of Group-1 where methane and sulfate co-occur with no indication of groundwater sulfate input and where sulfate reduction that surpasses sulfate addition from seawater (Fig. 2; Fig. A1). Data in Group-1 have positive net sulfate depletion rates indicative of sulfate reduction. The sulfate depletion is seen within the zone where methane concentrations are high. In these cores the net sulfate depletion rates can be used to derive the minimum methanogenesis rates (see model details in the Appendix). Reactions considered in this first approach include organic matter degradation via heterotrophic sulfate reduction, methane production via methanogenesis and methane addition from gas bubble dissolution (Haeckel et al., 2004; Chuang et al., 2013).

A second approach (detailed in the Appendix) was used for simulating the profiles for Group-2, Group-3 and Group-4 which show no positive net sulfate depletion rates when integrated over the core length. These sites are affected by groundwater input or by considerable irrigation and input of seawater. Here, the link between sulfate and methane reactions is less clear and hard to quantify directly.

The following equation was solved to quantify the rates of reaction and transport of dissolved methane and sulfate in the upper 20 cm of the sediments in both approaches (Berner, 1980; Boudreau, 1997):

$$\Phi \cdot \frac{\partial C}{\partial t} = \frac{\partial(\Phi \cdot D_s \frac{\partial C}{\partial x})}{\partial x} - \frac{\partial(\Phi \cdot v \cdot C)}{\partial x} + \Phi \cdot R_c \quad (2)$$

where  $x$  is sediment depth,  $t$  is time,  $\Phi$  is porosity,  $D_s$  is the solute-specific diffusion

**Deleted:** This is not expected and not typically observed since methanogenesis and sulfate reduction do not tend to co-exist because sulfate reduction is more energetically favorable than methanogenesis and anaerobic oxidation of methane (AOM) coupled with sulfate reduction occurs in sulfate containing environments. Previous research has shown that sulfate reducing microbes will out-compete methanogens for competitive substrates such as hydrogen and acetate, it is possible therefore that the high methane concentrations measured in sulfate rich porewater may be supplied by high rates of methanogenesis occurring at greater depths within the sediment below the sulfate reduction zone, or this may result from high abundance of competitive substrates in the sulfate reduction zone, hence reducing competition. The other possibility is that methanogens use various noncompetitive substrates. Indeed it has been reported that methanogens can use noncompetitive substrates, including methanol, trimethylamines and dimethylsulfide, in sulfate containing mangrove sediments and coastal lagoons. Our sediment slurry incubation experiments demonstrated that in sediments from Celestún the methanogenic community is capable of producing methane from a wide range of substrates, including: H<sub>2</sub>, acetate, formate, methanol, and trimethylamine (Fig. 5). Both methanol and trimethylamine are not utilized by sulfate reducers, which could allow methanogens to function at the same sediment depths as sulfate reducers (Fig. 5). The use of non-competitive substrates by the methanogenic community has important implications for methane flux to the atmosphere as it allows for methane production at shallow depths in the sediment reducing the potential for oxidation. Although processes and trends similar to those described above have been reported for other mangrove sediments the reports remain qualitative in nature. To better quantify the processes determining methane fluxes from mangrove sediments we use a transport-reaction model to simulate porewater data in these permanently submerged sediments.

**Deleted:** Transport-reaction model setting and model results of methane and sulfate dynamics in mangrove sediments

**Deleted:** rates

**Deleted:** s

**Deleted:** and

**Deleted:** we apply a transport-reaction model to simulate porewater data for profiles characterized by group-1 and group-2 trends where methane and sulfate co-occur (Fig. 2). Data for these two groups have positive net sulfate depletion rates indicative of sulfate reduction within the zone where methane concentrations are high. We also simulate net sulfate input and methane production/oxidation rates for data in group-3, group-4 and group-5. Reactions considered in the model include organic matter (expressed as CH<sub>2</sub>O in the equations below) degradation, organoclastic sulfate reduction (SR), methanogenesis, and anaerobic oxidation of methane (AOM). The following equations are used for these ... [3]

**Deleted:** s were

**Deleted:** rates of

**Deleted:** CH<sub>4</sub>

**Deleted:** SO<sub>4</sub><sup>2-</sup> and organic carbon (solid symbols; Fig. 4)

**Deleted:**

**Deleted:**

**Deleted:**

**Deleted:**

**Deleted:**

1 coefficient in the sediment,  $C$  is the concentration of methane or sulfate in the porewater,  $\gamma$  is  
 2 the burial velocity of porewater, and  $R_C$  is the sum of reactions affecting  $C$  (Table A1). Solutes  
 3 were simulated in moles  $L^{-1}$  of porewater (M). Details of all the reaction terms and parameters  
 4 and how they were derived for each of the approaches are given in the Appendix. The model  
 5 assumes steady state conditions to constrain methanogenesis rates at each site. Considering the  
 6 observed variability in porewater distributions non-steady state simulations would be desirable,  
 7 yet this would require continuous monitoring of porewater sulfate, methane and chloride  
 8 concentrations to evaluate temporal changes in sulfate depletion at each site. This time-series  
 9 data is unavailable, hence the modeled 'instantaneous' rates bear uncertainties that currently  
 10 cannot be quantified accurately.

11 Model derived sulfate depletion and sulfate and methane concentrations are shown in Fig. 2  
 12 and Fig. A1. Modeled porewater data for Group-1 (the most common trend) show that methane  
 13 generated from organic matter degradation within the upper sediments is a more important  
 14 methane source than methane diffusing from below and gas bubble dissolution, as further seen  
 15 in the results of ICEL\_Jul02 and the sensitivity analysis from 2CEL\_Jul02 (Fig. 5A). In  
 16 ICEL\_Jul02, for example, gas dissolution of methane transported from deeper sediments is not  
 17 necessary to achieve a good model fit to the data, and *in-situ* methanogenesis alone can  
 18 reproduce methane concentrations similar to the measured data even though methane  
 19 concentrations are oversaturated ( $> 1.1$  mM (in situ solubility)) (Fig. 2). In contrast, the  
 20 modeled methane profile for 2CEL\_Jul02 (black dashed line) arguably does require the  
 21 inclusion of methane from gas dissolution ( $R_{MB}$ ) (Fig. 5A). In Fig. 5A, the gray dashed and  
 22 solid lines represent only gas dissolution in the methane reaction terms (no methanogenesis  
 23 within the modeled 20 cm column) using different gas dissolution constants ( $k_{MB}$  values are  $0.2$   
 24  $yr^{-1}$  and  $0.5 yr^{-1}$  respectively). The model results shown as the gray dashed line simulate the  
 25 methane concentrations below 10 cm depth, whereas those shown by the gray solid line  
 26 reproduce methane concentrations in the upper 5cm, but neither reproduces the data throughout  
 27 the whole core. Comparing results considering methanogenesis and gas dissolution (black solid  
 28 line) and methanogenesis only (black dashed line), it is clear that both methanogenesis and  
 29 some gas dissolution are needed for reproducing the methane distribution in core 2CEL\_Jul02.  
 30 This illustrates the complexity of controlling processes and the dynamic nature and resulting  
 31 temporal variability in methane fluxes at this and the other sites in the lagoons.

### 5.3 Model derived depth-integrated turnover rates and fluxes

34 Table 2 lists the calculated depth-integrated turnover rates and fluxes for the individual cores.

- Deleted: solutes
- Deleted:  $G$  is the organic content in dry sediment,
- Deleted:  $w$  is the burial velocity of solids,
- Deleted: Sediment burial results in the downward movement of both sediment particles and porewater relative to the sediment water interface. Since we simulate  $[SO_4^{2-}]_{dep}$  to derive organoclastic sulfate reduction rates and  $[SO_4^{2-}]_{dep}$  is determined by seawater ( $[Cl^-]$ ) any upward advection of fluids (typically low in  $Cl$  and high in sulfate) was not included in model.
- Deleted: and organic contents in wt. % (d
- Deleted: shown
- Deleted: by using 5 years as the simulation time
- Deleted: are in Appendix A).
- Deleted:  $[SO_4^{2-}]_{dep}$
- Deleted:  $[SO_4^{2-}]$  and  $[CH_4]$
- Deleted: by solid and dashed lines, respectively.
- Deleted: in
- Deleted: g
- Deleted: sediments
- Deleted: active
- Deleted: than
- Deleted: ICEL\_Jul02 and
- Deleted: 6
- Deleted: in the core does
- Deleted: need to be included in the model
- Deleted: Indeed if we only consider gas dissolution without methanogenesis in the model for ICEL\_Jul02, the maximum methane that can be generated is not sufficient as depicted in the gray solid line because the maximum methane that can be dissolved from gas bubbles is 1.10 mM under the temperature, pressure and salinity of ICEL\_Jul02. ... [4]
- Deleted: methanogenesis ( $R_M$ )
- Deleted: ,
- Deleted: and anaerobic oxidation of methane ( $R_{AOM}$ )
- Deleted: The black solid line represents only  $R_M$  and ... [5]
- Deleted: solid and
- Deleted: and  $R_{AOM}$
- Deleted: column (
- Deleted: )
- Deleted: can fit
- Deleted: and
- Deleted: can fit
- Deleted:
- Deleted: actual
- Deleted: of the
- Deleted: (methanogenesis and gas dissolution combined)
- Deleted: the black dashed line (only
- Deleted: s
- Deleted: plus
- Deleted: both
- Deleted: .
- Deleted: modeled

1 For profiles in Group-1, methane sources include methanogenesis within the upper 20cm  
 2 and/or methane transported from deeper sections (>20cm) via bubble transport and dissolution.  
 3 Methane can be supported fully by methanogenesis without gas bubble dissolution within the  
 4 modeled upper 20cm in cores 1CEL\_Dec00, 1CEL\_Jul02, 1\_1CH\_Oct01 and 1\_2CH\_Oct01.  
 5 Gas bubble dissolution and transport from deeper sediments contributes more methane than  
 6 methanogenesis in cores 1CEL\_Apr00, 1CEL\_Oct01, 2CEL\_Dec00 and 3CEL\_Jul02.

7 Methane sinks include emissions to the water column or methane diffusion into deeper  
 8 sediments (>20 cm) and oxidation. Our model shows that the major sink for methane, however,  
 9 is emission to the water column accounting for over 90% of methane produced within the  
 10 upper 20 cm (e.g. 1CEL\_Apr00, 1CEL\_Oct01, 3CEL\_Apr00 and 3CEL\_Jul02). Model derived  
 11 methane fluxes to the water column are listed in Table 2 ( $F_{\text{methane (top)}}$ ) and range from 0.012-20  
 12  $\text{mmol CH}_4 \text{ m}^{-2} \text{ d}^{-1}$ . These are similar to or up to two orders of magnitude larger than fluxes  
 13 reported for other mangrove lagoon systems in Florida (0.02  $\text{mmol CH}_4 \text{ m}^{-2} \text{ d}^{-1}$ , Barber et al.,  
 14 1988; Harriss et al., 1988), Australia (0.03-0.52  $\text{mmol CH}_4 \text{ m}^{-2} \text{ d}^{-1}$ , Kreuzwieser et al., 2003),  
 15 and India (5.4-20.3  $\text{mmol CH}_4 \text{ m}^{-2} \text{ d}^{-1}$ , Purvaja and Ramesh, 2001). Since all methane depth  
 16 profile types were observed throughout the year with no differences in spatial and temporal  
 17 distribution (seasons and sampling locations), our results support the idea that methane fluxes  
 18 in coastal mangrove lagoon systems respond very dynamically to environmental stimuli.

19 Sulfate sinks include heterotrophic sulfate reduction and AOM, although the model suggests  
 20 that AOM plays a minor role compared to heterotrophic sulfate reduction. Sulfate reduction  
 21 ranges from 1.1 to 24  $\text{mmol SO}_4^{2-} \text{ m}^{-2} \text{ d}^{-1}$  and is the major sink for both sulfate and organic  
 22 carbon in most cores. Sulfate reduction accounts for 2.2 to 48  $\text{mmol C m}^{-2} \text{ d}^{-1}$  of total  
 23 anaerobic carbon respiration, which is in the same range of values listed in Kristensen et al.  
 24 (2008) for most mangrove sediments.

25 Mangrove forests are known to be highly productive systems with the capacity to release high  
 26 concentrations of dissolved organic matter (DOM) to surrounding sediments and porewaters  
 27 (Kristensen et al., 2008). Tree litter and subsurface root growth provide further significant  
 28 inputs of organic carbon to mangrove sediments which are unique for this type of system. The  
 29 rate of organic matter mineralization ( $R_{\text{POC}}$ ; Eq. A6) derived from sulfate depletion ranges from  
 30 3.2  $\text{mmol C m}^{-2} \text{ d}^{-1}$  to 110  $\text{mmol C m}^{-2} \text{ d}^{-1}$ . Although our modeling approach for determining  
 31 degradation rates is not without uncertainty, it is more accurate than rates derived from  
 32 down-core trends in organic matter content because of temporal variability in accumulation  
 33 rates in this area (Gonneea et al., 2004). Particulate organic matter will also contain a high  
 34 amount of refractory carbon that is not easy to quantify and separate from the bulk pool. The  
 35 derived degradation rates likely represent the more labile particulate components and labile

Deleted: Results f

Deleted: group

Deleted: or diffusion

Deleted:

Deleted: are AOM, methane

Deleted: Less than 5% of methane was consumed by AOM showing that AOM is the minor sink for methane for cores in group-1. T

Deleted:

Deleted: methane

Deleted: sediment column

Deleted: organoclastic

Deleted: anaerobic oxidation of methane (

Deleted: );

Deleted: .

Deleted: our

Deleted: but

Deleted: also

Deleted: for

Deleted: Organoclastic s

Deleted: .

Deleted: ranging

Deleted:  $\text{mmol SO}_4^{2-} \text{ m}^{-2} \text{ d}^{-1}$

Deleted: .

Deleted: If organoclastic s

Deleted: reduction is converted to C units this process can

Deleted: -50

Deleted: in the model

Deleted: inorganic C release;

Deleted: that reported

Deleted: .

Deleted: Specifically in this system there are indications for additional sulfate inputs to the porewater (low Cl high sulfate groundwater) hence the calculated net sulfate reaction rates ( $F_{\text{sulfate (net)}}$ ) are underestimated of the actual reduction rates (e.g. cores 1CEL\_Dec00, 1CEL\_Oct01, 2CEL\_Dec00 and 2CEL\_Jul02).

Deleted: relying

Deleted: on

Deleted: the measured organic matter content in this area shows evidence for

1 DOM that was not considered (or measured) in this study. The high calculated organic carbon  
 2 oxidation rates derived here are thus not unexpected since mangrove systems in general (e.g.  
 3 Dittmar et al., 2006; Dittmar and Lara, 2001; Lee 1995; Odum and Heald, 1975) and the  
 4 lagoons in Yucatan in particular are dominated by high concentrations of DOM, a large fraction  
 5 of which is likely to be labile (Young et al., 2005).

6 Depth-integrated methane production or consumption rates ( $R_{CH_4}$ ) and net sulfate inputs  
 7 ( $R_{SO_4^{2-}}$ ) calculated from Eqs. (A9) and (A10) for cores in Group-2, Group-3 and Group-4 are  
 8 listed in Table 2. The methane and sulfate net production/consumption rates ranged from  
 9 -0.060 to +11 mmol CH<sub>4</sub> m<sup>-2</sup> d<sup>-1</sup> and -69 to +21 mmol SO<sub>4</sub><sup>2-</sup> m<sup>-2</sup> d<sup>-1</sup>. (Negative values indicate  
 10 net sulfate or methane consumptions while positive values indicate production or addition from  
 11 external sources). Although sulfate depletion values for cores in Group-2 are positive (e.g. net  
 12 sulfate reduction), sulfate concentrations at some depths of the porewater are relatively high,  
 13 suggesting continuous sulfate input from deeper within the sediments or from seawater. Cores  
 14 in Group-3 and Group-4 show negative or zero sulfate depletion that likely results from sulfate  
 15 addition from groundwater (Group-3) or seawater (Group-4), thus prohibiting accurate  
 16 calculation of sulfate reduction and methanogenesis rates. Although, in theory, H<sub>2</sub>S oxidation is  
 17 a possible source for the excess sulfate, we believe that sulfate-rich groundwater input is a  
 18 more likely source due to correlation between excess sulfate and excess Sr which has been  
 19 previously described for groundwater in this region (Young et al., 2008). Perry et al. (2002)  
 20 identified dissolution of evaporites within the freshwater lens at some Yucatán sites as a  
 21 probable source of excess sulfate in groundwater using the sulfate-to-chloride ratio  
 22 (100×(SO<sub>4</sub>/Cl)). Ratios higher than seawater (average seawater is 10.3) are expected where  
 23 gypsum/anhydrite dissolution occurs (Perry et al. 2002). Another indicator is the Sr/Cl ratio,  
 24 which is invariably higher in the Yucatan groundwater than in seawater and indicates  
 25 dissolution of celestite (from evaporite) and/or aragonite (Perry et al., 2002). The region east  
 26 and south of Lake Chichancanab, referred to as the Evaporite Region by Perry et al. (2002), is  
 27 characterized by distinctive topography and high sulfate groundwater concentrations (Perry et  
 28 al., 2002). The groundwater from the Lake Chichancanab area flows northward into the  
 29 Celestún Estuary which can be recognized by the progressive decrease in the ratio  
 30  $\frac{[\frac{SO_4}{Cl}]_{groundwater}}{[\frac{SO_4}{Cl}]_{seawater}}$  in water from southeast to northwest (Perry et al., 2009). The Sr and sulfur  
 31 trends for Celestún lagoon (Young et al., 2008) are consistent with our interpretation that  
 32 gypsum/anhydrite dissolution in groundwater is the source of excess sulfate in the porewater of  
 33 Group-3 in Celestún lagoon. Due to the impact of groundwater, our sulfate reduction and  
 34 methanogenesis rates estimated using the model are minimum rates and independent rates of

**Deleted:** Organoclastic sulfate reduction and methanogenesis derived from the rate of organic matter mineralization range from 3.4 mmol C m<sup>-2</sup> d<sup>-1</sup> to 113 mmol C m<sup>-2</sup> d<sup>-1</sup>. However, the organic matter content in the sediments increase with depth and accumulates in the deeper sediments, inconsistent with expected consumption trends (Fig. 4). Organic carbon degradation rates for data in Fig. 4 were quantified by . Results show negative values which means organic carbon accumulates and is buried in the deeper sediments (as observed) (Table 2). Organic carbon burial rates derived from the model for both lagoons (Table 2) are in the same range as those reported in (9-16 mmol C m<sup>-2</sup> d<sup>-1</sup> in Celestún Lagoon and 15-24 mmol C m<sup>-2</sup> d<sup>-1</sup> in Chelem Lagoon). The measured organic carbon content may contain high amount of refractory carbon yet the degradation rates (R<sub>POC</sub>; Eq. A7) converted from sulfate depletion rates likely represent the more labile organic carbon pool which is no longer present in the sediment or dissolved organic matter which was not considered (or measured) in this study. A wide range of substrates, including: H<sub>2</sub>, acetate, formate, methanol, and trimethylamine which are not included in the sedimentary organic matter measured in the core can be utilized for methane production and/or sulfate reduction (Fig. 2) the high calculated organic carbon oxidation rates are therefore not surprising. Indeed mangrove systems in general (e.g. and the lagoons in Yucatan in particular are dominated by high DOC. Although the (1-f<sub>SO4</sub>) term in Eq. (A8) may indicate that methanogenesis is inhibited by sulfate (R<sub>M</sub> is from competitive substrates) it can also be explained as the portion of organic carbon degradation (R<sub>M</sub>) from non-competitive substrates within the modeled length. Methane concentrations are not reproduced as well for cores in group-2 (in comparison to group-1) in our model. No methanogenesis is seen in the upper sediments as suggested by the negative value of F<sub>SR</sub>. Different ... [6]

<b>Deleted:</b> F
<b>Deleted:</b> F
<b>Deleted:</b> A12
<b>Deleted:</b> A13
<b>Deleted:</b> group
<b>Deleted:</b> 3
<b>Deleted:</b> g
<b>Deleted:</b> 4
<b>Deleted:</b> g
<b>Deleted:</b> 5
<b>Deleted:</b> M
<b>Deleted:</b> 0.012
<b>Deleted:</b> -
<b>Deleted:</b> 0.83-10
<b>Deleted:</b> .
<b>Deleted:</b>
<b>Deleted:</b> occurs
<b>Deleted:</b> values
<b>Deleted:</b> ing
<b>Deleted:</b> sulfate domination
<b>Deleted:</b> limiting the ability to
<b>Deleted:</b> ly
<b>Deleted:</b> c
<b>Deleted:</b> is involved
<b>Deleted:</b> , Mexico

1 groundwater discharge into each core are needed for obtaining more realistic estimates in these  
2 sites.

3 In addition to depth-integrated rates, Table 3 also includes maximum methanogenesis/methane  
4 production ( $Max-R_M$ ) and sulfate reduction/consumption ( $Max-R_{SR}$ ) rates solved by Eq. 2 in the  
5 model. Interestingly, the maximum methane production rates estimated from TMA, methanol  
6 and  $H_2$  additions to sediments in the slurry incubations (Table 1) are similar to model derived  
7  $Max-R_M$  at station 16CEL (Table 3), which is the site from which sediments were collected for  
8 the slurry incubations. The rates in the TMA, methanol and  $H_2$  treatments from the slurry  
9 incubations (Table 1) and in some of our stations are higher than methane production rates  
10 from previously reported coastal freshwater and brackish wetland sediments that were  
11 measured using radiolabeled acetate and bicarbonate in slurries (Segarra et al., 2013).

12 Modeled  $Max-R_M$  in some cores were 1-2 orders of magnitude higher than rates derived from  
13 the sediment slurry incubations (e.g., cores 1CEL\_Jul02, 1\_1CH\_Oct01, 2CEL\_Oct01 and  
14 14CEL\_Dec00). Although heterotrophic sulfate reduction generally dominates organic matter  
15 degradation,  $Max-R_M$  values are even higher than the maximum sulfate reduction rates in some  
16 cores (1\_1CH\_Oct01, 1\_2CH\_Oct01 and 1CH\_Dec00). Both the methanogenesis rates  
17 measured in the sediment slurry incubations and the modeled maximum methanogenesis rates  
18 in this study area were much higher than those reported for some mangrove systems (e.g.,  
19 Thailand, Kristensen et al., 2000; Malaysia, Alongi et al., 2004; Australia, Kristensen and  
20 Alongi, 2006) but similar to other sites in India (Ramesh et al., 2007).

21 AOM is expected to play an important role in tropical porewaters with abundant methane and  
22 sulfate (Biswas et al., 2007). However, our model results and sensitivity analyses indicate that  
23 AOM is insufficient to prevent methane escape to the bottom water, probably because of the  
24 abundant organic matter available for sulfate reducers to use instead of methane. In our  
25 sensitivity tests (using core 1CEL\_Oct01 as an example), if AOM is allowed to be responsible  
26 for sulfate and methane consumption (no heterotrophic sulfate reduction and methanogenesis;  
27  $R_{SD}=R_{AOM}$ ) then methane concentrations would decrease to negative values (gray solid lines in  
28 Fig. 5B), which is inconsistent with observations. Although based on our data it is not possible  
29 to accurately quantify the relative proportion of sulfate loss due to heterotrophic sulfate  
30 reduction and/or AOM, our model results suggest AOM plays a minor role in this setting.  
31 Future investigations on the role of AOM in these dynamic mangrove-dominated tropical  
32 coastal lagoons are needed (e.g., Thalasso et al, 1997; Raghoebarsing et al., 2006; Lee et al.,  
33 2008; Kristensen et al., 2008; Beal et al., 2009; Silvan et al., 2011; Segarra et al., 2013).

Deleted: values of

Deleted: ;

Deleted: this

Deleted: reaches

Deleted: such as

Deleted: we allow

Deleted: ;

Deleted: this

Deleted: im

Deleted: AOM plays a minor role in cores in group-3, group-4 and group-5 like in groups 1 and 2. Although specific sources of methane and sulfate can't be identified using this approach independent studies suggest that sulfate can be added from external sources specifically groundwater in this region. The major sink for methane in these cores is methane emission to the water.

## 1 6 Conclusions

2 The variable trends observed in porewater chemistry indicate a very dynamic system spatially  
3 and temporally throughout the year. This can be explained by physical processes such as  
4 mixing and dilution with seawater or groundwater, gas bubble rise and dissolution and  
5 microbial processes which operate at different rates during different times at all sites. Although  
6 our modeling suggests that organic carbon degradation rates are dominated by heterotrophic  
7 sulfate reduction in these cores, methanogenesis both in shallow and deeper sediments is  
8 prevalent. The co-occurrence of methane and sulfate reduction (documented by sulfate  
9 depletion) in shallow sediments of non-competitive substrates and ample dissolved and labile  
10 organic matter in the shallow sediments as well as the contributions of methane from deeper  
11 sediment through gas rise and dissolution. Model results demonstrate that the largest sink for  
12 methane in these sediments is efflux to the water column. Build-up of methane at shallow  
13 depths may reduce the fraction of methane that is oxidized prior to entering the water column,  
14 thereby increasing the flux at the sediment-water interface. This shallow methane pool may  
15 also encourage methane flux through bubble release, which can result in a larger fraction of the  
16 methane reaching the atmosphere without being lost to oxidation. Specifically, the ability of  
17 the microbial community in these sediments to use non-competitive substrates may allow for  
18 methane production in the upper sections of the sediment potentially contributing to the higher  
19 than expected atmospheric methane flux measured from mangrove-dominated tropical coastal  
20 lagoons.

21  
22 **Appendix: Modeling procedure used in the evaluation of porewater observations from**  
23 **sediments in mangrove-dominated tropical coastal lagoons, Yucatán, Mexico**

24 Details of the modeling procedure and parameters used are described here. The following  
25 reactions are considered in the model:

26  
27 Heterotrophic sulfate reduction ( $R_{SR}$ ):



29  
30 Methanogenesis ( $R_M$ ):  $2\text{CH}_2\text{O} \rightarrow \text{CO}_2 + \text{CH}_4$  (R2)

31  
32 Gas bubble dissolution ( $R_{MB}$ ):  $\text{CH}_4(\text{g}) \rightarrow \text{CH}_4(\text{aq})$  (R3)

33  
34 The net reaction terms ( $R_C$  in Eq. 2) are given in Table A1, boundary conditions are listed in

Deleted: and

Deleted: different rates of operation of

Deleted:

Deleted: and biological processes (bacterial methane production and methane and sulfate consumption)

Deleted: organoclastic

Deleted:

Deleted: in this system is explained by high methane production rates supported by

Deleted: bubbles dissolution and diffusion

Deleted: AOM is a minor sink for sulfate and methane.

Deleted: The major sink for

Deleted: methane

Deleted: to the atmosphe

Deleted: , and it may

Deleted: also

Deleted: produced

Deleted: contribute to the higher than expected atmospheric methane flux measured from these mangrove lagoons. .

Deleted: Appendix A: Modeling procedure used in the evaluation of the mangrove-dominated tropical coastal lagoons, Yucatán, Mexico data

1 Table A2, best-fit model parameters are given in Table A3 and model derived concentration  
2 profiles are shown in Fig. 2 and Fig. A1.

3 In Eq. (2), sediment porosity decreases with depth due to steady-state compaction:

$$\Phi = \Phi_f + (\Phi_0 - \Phi_f) \cdot e^{-px} \quad (A1)$$

7 where  $\Phi_f$  is the porosity below the depth of compaction (0.78 for Celestún and 0.83 for  
8 Chelem),  $\Phi_0$  is porosity at the sediment surface (0.90 for Celestún and 0.89 for Chelem) and  $p$   
9 ( $1/15 \text{ cm}^{-1}$ ) is the depth attenuation coefficient. These parameters were determined from the  
10 measured porosity data at each site or at a nearby site (Eagle, 2002).

11 Under the assumption of steady state compaction, the burial of porewater was calculated as in  
12 (Wallmann et al. 2006):

$$v = \frac{\Phi_f \cdot w_f}{\phi} \quad (A2)$$

17 where  $w_f$  is the sedimentation rate of compacted sediments calculated from excess  $^{210}\text{Pb}$  data  
18 ( $0.25 \text{ cm/yr}$  for Celestún and  $0.35 \text{ cm/yr}$  for Chelem; Gonnee et al. (2004)). Sediment burial  
19 results in the downward movement of both sediment particles and porewater relative to the  
20 sediment water interface.

21 The sediment diffusion coefficient of each solute ( $D_s$ ) was calculated according to Archie's law  
22 considering the effect of tortuosity on diffusion (Boudreau 1997):

$$D_s = \Phi^2 \cdot D_M \quad (A4)$$

26 where  $D_M$  is the molecular diffusion coefficient at the in situ temperature, salinity and pressure  
27 (Table A1) calculated according to (Boudreau 1997). We used the same tortuosity coefficient  
28 ( $\Phi^2$  corresponding to  $m = 3$  in Archie's law) as reported by Wallmann et al. (2006) for  
29 fine-grained sediments.

30 Since net sulfate consumption is observed in Groups 1 profiles (Fig. 2; Fig. A1), we use the  
31 following calculations to obtain net sulfate depletion rates ( $R_{SD}$ ;  $\text{mmol SO}_4^{2-} \text{ cm}^{-3} \text{ yr}^{-1}$ ).  $R_{SD}$  is  
32 proportional to the difference between modeled ( $C(\text{SO}_4^{2-})_{dep}$ ) and measured concentrations  
33 ( $C(\text{SO}_4^{2-})_{OBS}$ ):

**Deleted:** Details of the modeling procedure and parameters are described in the following equations and Table A1-A3. In Eqs. (2) and (3), sediment porosity decreases with depth due to steady-state compaction: .

**Deleted:** of porosity

**Deleted:** advection of fluids

**Deleted:**  $w = \frac{(1-\Phi_f)w_f}{(1-\Phi)}$

**Deleted:** dating of sediments

**Deleted:** The net reaction terms ( $R_C$  in Eq. A2) of modeled species are given in Table A2 and boundary conditions used in the model are listed in Table A3. .

**Deleted:** groups

**Deleted:** and 2

**Deleted:** .

**Deleted:** We

**Deleted:** which are set to be

**Deleted:** .

**Moved down [1]:** The corresponding kinetic constant is set to be high ( $k_{SD} = 100\text{-}500 \text{ yr}^{-1}$ ) so that concentrations calculated in the model are always very close to measured values.

**Deleted:** .

1  
2  
3  
4  
5  
6  
7  
8  
9  
10  
11  
12  
13  
14  
15  
16  
17  
18  
19  
20  
21  
22  
23  
24  
25  
26  
27  
28  
29  
30  
31  
32

$$R_{SD} = k_{SD} \cdot \left( c(SO_4^{2-}{}_{dep})_{OBS} - c(SO_4^{2-}{}_{dep}) \right) \quad (A4)$$

The corresponding kinetic constant is set to be high ( $k_{SD} > 100 \text{ y}^{-1}$ ) to ensure that simulated concentrations are very close to measured values.

$R_{SD}$  implicitly includes  $R_{SR}$  as well as anaerobic oxidation of methane ( $R_{AOM}$ ):



The numerical modeling procedure outlined in Wallmann et al. (2006) is used as a basis to simulate the rate of sedimentary organic carbon degradation ( $R_{POC}$ ) by sulfate reduction and methanogenesis. Since the measured organic matter content in both lagoons showed evidence for a change in depositional pattern over time (Gonneea et al., 2004 and Eagle, 2002), these measurements cannot be used for reliable organic matter degradation calculations. Hence,  $R_{SR}$  (Eq. A5 below) was first calculated and then used to estimate  $R_{POC}$  (Eq. A6) and subsequently to derive  $R_M$  (Eq. A7). Here, we assume the three reactions (R1, R2 and R4) co-occur in the sulfate reduction zone such that the net reaction for methanogenesis and AOM (reactions R2+R4) is equal to carbon respiration by heterotrophic sulfate reduction (reaction R1). In other words,  $R_{SD} = 0.5R_{POC}$ .

To approximate the fraction of  $R_{POC}$  due to  $R_M$  and  $R_{SR}$ , a Michaelis-Menten kinetic limitation term is applied to Eq. (A5-A7) (Wallmann et al., 2006):

$$R_{SR} = R_{SD} = 0.5 \cdot R_{POC} \cdot f_{SO_4^{2-}} \quad (A5)$$

$$R_{POC} = \frac{R_{SD}}{0.5 \cdot f_C \cdot f_{SO_4^{2-}}} \quad (A6)$$

$$R_M = 0.5 \cdot f_C \cdot R_{POC} \cdot (1 - f_{SO_4^{2-}}) \quad (A7)$$

where  $f_{SO_4^{2-}} = \frac{c_{SO_4^{2-}}}{c_{SO_4^{2-}} + K_{SR}}$  is the Michaelis-Menten rate-limiting term for sulfate reduction.

At sites where methanogenesis was insufficient to simulate the measured methane data, methane was added as an external source by dissolution of gas bubbles (Chuang et al., 2013).

Deleted: (  
Deleted:  $c(SO_4^{2-}{}_{dep})_{OBS} - c(SO_4^{2-}{}_{dep})$   
Deleted: 5  
Moved (insertion) [1]  
Deleted: =  
Deleted: -500  
Deleted: so  
Deleted:  
Deleted: calculated in the model  
Deleted: always

Deleted: In Wallmann et al. (2006), Michaelis-Menten kinetic limitation terms were used to define how the rate of organic carbon degradation ( $R_{POC}$ ) is coupled to rate of organoclastic sulfate reduction ( $R_{SR}$ ) and methanogenesis ( $R_M$ ).  $R_{SR}$  is obtained by Eq. (A5) for sites where  $[SO_4^{2-}{}_{dep}]_{OBS}$  is positive. Since AOM may play a minor role in the methane and sulfate rich sediment and  $R_{AOM}$  was included in the net reaction rates of methane and sulfate this is justified. ... [7]  
Deleted: - ... [8]  
Deleted: )  
Deleted: A8

Gas bubbles were observed in the field. The rate of dissolution of the gas bubbles ( $R_3$ ) rising through the sediment ( $\text{CH}_{4(g)} \rightarrow \text{CH}_4$ ) was also considered as (Haeckel et al., 2004):

$$R_{MB} = k_{MB} \cdot (L_{MB} - C_{CH_4}) \quad \text{if } CH_4 \leq L_{MB} \quad (A8)$$

where  $L_{MB}$  is the in situ methane gas solubility concentration calculated using the algorithm of (Duan et al., 1992a; Duan et al., 1992b) and the site-specific salinity, temperature and pressure.  $R_{MB}$  depends on the first-order rate constant  $k_{MB}$ , which is a fitting parameter that lumps together gas dissolution in addition to diffusion of dissolved gas in the bubble tubes and walls.

Since sulfate depletion profile trends in Group-2, Group-3 and Group-4 show evidence of groundwater or seawater input with no positive depth integrated net sulfate depletion rates, the second approach for determining net methane and sulfate reaction rates for porewater data in these three groups is summarized as:

$$R_{CH_4} = k_{CH_4} \cdot (C_{CH_4OBS} - C_{CH_4}) \quad (A9)$$

$$R_{SO_4^{2-}} = k_{SO_4^{2-}} \cdot (C_{SO_4^{2-}OBS} - C_{SO_4^{2-}}) \quad (A10)$$

Net methane and sulfate reaction rates are set to be proportional to the difference between modeled ( $C_{CH_4}$  and  $C_{SO_4^{2-}}$ ) and measured concentrations ( $C_{CH_4OBS}$  and  $C_{SO_4^{2-}OBS}$ ). The corresponding kinetic constant  $k_{CH_4}$  and  $k_{SO_4^{2-}}$  are listed in Table A3.

Methane fluxes at the boundaries were calculated using the model as follows:

$$F_{CH_4}(x) = \Phi(x) \cdot \left( v(x) \cdot C_{CH_4} - D_S \cdot \frac{dC_{CH_4}(x)}{dx} \right) \quad (A11)$$

where  $x = 20$  cm is the bottom of the simulated core and  $x = 0$  cm is the sediment-water interface.

Fixed concentrations were imposed for all solutes at the upper and lower boundaries to values measured at or near the sediment-water interface and at 20 cm. The method-of-lines was used to transfer the set of finite difference equations of the spatial derivatives of the coupled partial differential equations to the ordinary differential equation solver (NDSolve) in MATHEMATICA v. 7.0, using a grid spacing which increased from ca. 0.015 cm at the

**Deleted:** The rate of AOM ( $R_{AOM}$ ) was simulated using bimolecular kinetics (Regnier et al. 2011): - ... [9]

**Deleted:** - ... [10]

**Deleted:**  $\text{CH}_{4(g)} \rightarrow \text{CH}_4$  if  $\text{CH}_4 \leq L_{MB}$  ( $R_4$ ) -

**Deleted:** Methane dissolution ( $R_{MB}$ ):

**Deleted:**  $\Delta 10$

**Deleted:**

**Deleted:** of the bottom water. The rate of gas dissolution ( **Deleted:** )

**Deleted:** the difference between  $L_{MB}$  and the in situ methane concentration using a

**Deleted:** -

**Deleted:**  $k_{MB}$

**Deleted:** the rate of

**Deleted:** We use the same approach as that used for obtaining sulfate depletion rates ( $R_{SD}$ ) to calculate organic carbon degradation ( $C_{organic}$ ) rates in cores 2CEL\_Dec00, 3CEL\_Dec00, 1CH\_Dec00 and 1CH\_Oct01 (Fig. 4) where organic carbon data is available. -

Net methane and sulfate reaction rates for porewater data in group-3, group-4 and group-5 are expressed as: -

**Deleted:** Net methane and sulfate reaction rates for group-3, group-4 and group-5 are expressed as: -

**Deleted:** 13

**Deleted:** 4

**Deleted:** In Eqs. (A12) and (A13),

**Deleted:** ( $R_{CH_4}$  and  $R_{SO_4^{2-}}$ )

**Deleted:**  $\Delta 1$

**Deleted:** AOM rates are estimated via Eq. (A9) by using the modeled methane and sulfate concentrations from Eqs. (A12) and (A13).

**Deleted:** -

**Deleted:** which were set

**Deleted:** All models were run for  $1 \times 10^6$  yr to achieve steady state

1 sediment surface to 0.38 cm at depth. Since most of the porewater profiles were fitted directly,  
2 only a few years of simulation time (5 yr) was needed to achieve steady state. Mass balance  
3 was typically better than 99.9%.

Deleted: 5

#### 5 **Acknowledgements**

6 We thank the staff of the DUMAC Celestún station and the students of CINVESTAV for  
7 assistance with laboratory space, lodging, and field work. We thank Tom Lorenson and Ron  
8 Oremland of the Menlo Park, CA USGS for facility use and analyses for slurry  
9 incubations. This work was funded by Consejo Nacional de Ciencia y Tecnología Ref: 4147-P  
10 T9608, 32356T, and CONABIO Ref: B019 to J H-S, NSF INT 009214214 to AP, a Stanford  
11 Graduate Fellowship and Lieberman Fellowship to MY and a fellowship of the Postdoctoral  
12 Research Abroad Program, sponsored by the National Science Council, Taiwan to PCC (now:  
13 MOST (the Ministry of Science and Technology)). We thank John Pohlman and an anonymous  
14 reviewer for their thoughtful comments and the associate editor (Helge Niemann) for handling  
15 the manuscript.

Deleted: and

#### 17 **References**

- 18 Alongi, D. M., Sasekumar, A., Chong, V. C., Pfitzner, J., Trott, L. A., Tirendi, F., Dixon, P., and  
19 Brunskill, G. J.: Sediment accumulation and organic material flux in a managed mangrove  
20 ecosystem: estimates of land–ocean–atmosphere exchange in peninsular Malaysia, *Marine*  
21 *Geology*, 208, 383-402, 2004.
- 22 Alongi, D. M., Pfitzner, J., Trott, L. A., Tirendi, F., Dixon, P., and Klumpp, D. W.: Rapid  
23 sediment accumulation and microbial mineralization in forests of the mangrove *Kandelia*  
24 *candel* in the Jiulongjiang Estuary, China, *Estuar. Coast. Shelf S.*, 63, 605–618, 2005.
- 25 Barber, T. R., Burke, R. A., and Sackett, W. M.: Di<sub>2</sub> flux of methane from warm wetlands,  
26 *Global Biogeochem. Cy.*, 2, 411–425, 1988.
- 27 Barnes, J., Ramesh, R., Purvaja, R., Nirmal Rajkumar, A., Senthil Kumar, B., Krithika, K.,  
28 Ravichandran, K., Uher, G., and Upstill-Goddard, R.: Tidal dynamics and rainfall control N<sub>2</sub>O  
29 and CH<sub>4</sub> emissions from a pristine mangrove creek, *Geophys. Res. Lett.*, 33, L15405,  
30 doi:10.1029/2006GL026829, 2006.
- 31 Bartlett, K. B., Harriss, R. C., and Sebacher, D. I.: Methane flux from coastal salt marshes, *J.*  
32 *Geophys. Res.-Atmos.*, 90, 5710–5720, 1985.
- 33 Bartlett, K. B., Bartlett, D. S., Harriss, R. C., and Sebacher, D. I.: Methane emissions along a

- 1 salt marsh salinity gradient, *Biogeochemistry*, 4, 183–202, 1987.
- 2 [Beal, E. J., House, C. H., and Orphan, V. J.: Manganese- and Iron-Dependent Marine Methane](#)  
3 [Oxidation, \*Science\*, 325, 184-187, 2009.](#)
- 4 Berner, R. A.: *Early Diagenesis. A Theoretical Approach*, Princeton University Press, Princeton,  
5 NJ, USA, 241 pp., 1980.
- 6 Biswas, H., Mukhopadhyay, S. K., De, T. K., Sen, S., and Jana, T. K.: Biogenic controls on the  
7 air-water carbon dioxide exchange in the Sundarban mangrove environment, northeast coast of  
8 Bay of Bengal, India, *Limnol. Oceanogr.*, 49, 95–101, 2004.
- 9 Biswas, H., Mukhopadhyay, S. K., Sen, S., and Jana, T. K.: Spatial and temporal patterns of  
10 methane dynamics in the tropical mangrove dominated estuary, NE coast of Bay of Bengal,  
11 India, *J. Marine Syst.*, 68, 55–64, 2007.
- 12 Boudreau, B. P.: *Diagenetic Models and Their Implementation: Modelling Transport and*  
13 *Reactions in Aquatic Sediments*, Springer-Verlag, Berlin, 414 pp., 1997.
- 14 Call, M., Maher, D. T., Santos, I. R., Ruiz-Halpern, S., Mangion, P., Sanders, C. J., Erler, D. V.,  
15 Oakes, J. M., Rosentreter, J., Murray, R., and Eyre, B. D.: Spatial and temporal variability of  
16 carbon dioxide and methane fluxes over semi-diurnal and spring–neap–spring timescales in a  
17 mangrove creek, *Geochim. Cosmochim. Ac.*, 150, 211–225, 2015.
- 18 Capone, D. G. and Kiene, R. P.: Comparison of microbial dynamics in marine and freshwater  
19 sediments: contrasts in anaerobic carbon catabolism, *Limnol. Oceanogr.*, 33, 725–749, 1988.
- 20 Chuang, P.-C., Dale, A. W., Wallmann, K., Haeckel, M., Yang, T. F., Chen, N.-C., Chen, H.-C.,  
21 Chen, H.-W., Lin, S., Sun, C.-H., You, C.-F., Horng, C.-S., Wang, Y., and Chung, S.-H.:  
22 Relating sulfate and methane dynamics to geology: accretionary prism on shore SW Taiwan,  
23 *Geochem. Geophys. Geosy.*, 14, 2523–2545, 2013.
- 24 Dittmar, T. and Lara, R. J.: Driving forces behind nutrient and organic matter dynamics in a  
25 mangrove tidal creek in North Brazil, *Estuar. Coast. Shelf S.*, 52, 249–259, 2001.
- 26 Dittmar, T., Hertkorn, N., Kattner, G., and Lara, R. J.: Mangroves, a major source of dissolved  
27 organic carbon to the oceans, *Global Biogeochem. Cy.*, 20, GB1012,  
28 doi:10.1029/2005GB002570, 2006.
- 29 Duan, Z., Møller, N., Greenberg, J., and Weare, J. H.: The prediction of methane solubility in  
30 natural waters to high ionic strength from 0 to 250 °C and from 0 to 1600 bar, *Geochim.*  
31 *Cosmochim. Ac.*, 56, 1451–1460, 1992a.
- 32 Duan, Z. H., Møller, N., and Weare, J. H.: An equation of state for the CH<sub>4</sub>-CO<sub>2</sub>-H<sub>2</sub>O

1 system. I. pure systems from 0 °C to 1000 °C and 0 to 8000 bar, *Geochim. Cosmochim. Acta.*,  
2 56, 2605–2617, 1992b.

3 [Eagle, M.: Tracing organic matter sources in mangrove estuaries utilizing  \$\delta^{13}\text{C}\$ ,  \$\delta^{15}\text{N}\$  and C/N](#)  
4 [Ratios. Master Thesis, Stanford University, Stanford, CA, USA, 2002.](#)

5 [Ferdelman, T. G., Lee, C., Pantoja, S., Harder, J., Bebout, B. M., and Fossing, H.: Sulfate](#)  
6 [reduction and methanogenesis in a Thioploca-dominated sediment off the coast of Chile,](#)  
7 [Geochimica et Cosmochimica Acta, 61, 3065-3079, 1997.](#)

8 Fung, I., John, J., Lerner, J., Matthews, E., Prather, M., Steele, L. P., and Fraser, P. J.:  
9 Threedimensional model synthesis of the global methane cycle, *J. Geophys. Res.-Atmos.*, 96,  
10 13033–13065, 1991.

11 Gonnee, M. E., Paytan, A., and Herrera-Silveira, J. A.: Tracing organic matter sources and  
12 carbon burial in mangrove sediments over the past 160 years, *Estuar. Coast. Shelf S.*, 61,  
13 211–227, 2004.

14 ~~Haeckel, M., Suess, E., Wallmann, K., and Rickert, D.: Rising methane gas bubbles form~~  
15 ~~massive hydrate layers at the seafloor, *Geochim. Cosmochim. Acta.*, 68, 4335–4345, 2004.~~

16 [Harriss, R. C., Sebacher, D. I., Bartlett, K. B., Bartlett, D. S., and Crill, P. M.: Sources of](#)  
17 [atmospheric methane in the south Florida environment, \*Global Biogeochemical Cycles\*, 2,](#)  
18 [231-243, 1988.](#)

19 Herrera-Silveira, J. A.: Nutrients from underground discharges in a coastal lagoon (Celestún,  
20 Yucatán, México), *Verhandlungen des Internationalen Verein Limnologie*, 25, 1398–1403,  
21 1994.

22 Herrera-Silveira, J. A., Ramírez R, J., and Zaldivar R, A.: Overview and characterization of the  
23 hydrology and primary producer communities of selected coastal lagoons of Yucatán, México,  
24 *Aquatic Ecosystem Health and Management*, 1, 353–372, 1998.

25 Holmer, M. and Kristensen, E.: Coexistence of sulfate reduction and methane production in an  
26 organic-rich sediment, *Mar. Ecol.-Prog. Ser.*, 107, 177–184, 1994.

27 [Jørgensen, B. B. and Kasten, S.: Sulfur Cycling and Methane Oxidation. In: \*Marine\*](#)  
28 [Geochemistry, Schulz, H. D. and Zabel, M. \(Eds.\), Springer Berlin Heidelberg, Berlin,](#)  
29 [Heidelberg, 2006.](#)

30 [Kreuzwieser, J., Buchholz, J., and Rennenberg, H.: Emission of Methane and Nitrous Oxide by](#)  
31 [Australian Mangrove Ecosystems, \*Plant Biology\*, 5, 423-431, 2003.](#)

32 [Kristensen, E., Andersen, F. Å., Holmboe, N., Holmer, M., and Thongtham, N.: Carbon and](#)

**Deleted:** Gonnee, M. E., Charette, M. A., Liu, Q.,  
Herrera-Silveira, J. A., and Morales-Ojeda, S. M.: Trace  
element geochemistry of groundwater in a karst subterranean  
estuary (Yucatan Peninsula, Mexico), *Geochim.  
Cosmochim. Acta.*, 132, 31–49, 2014.

- 1 [nitrogen mineralization in sediments of the Bangrong mangrove area, Phuket, Thailand,](#)  
2 [Aquatic Microbial Ecology, 22, 199-213, 2000.](#)
- 3 [Kristensen, E. and Alongi, D. M.: Control by fiddler crabs \(\*Uca vocans\*\) and plant roots](#)  
4 [\(\*Avicennia marina\*\) on carbon, iron, and sulfur biogeochemistry in mangrove sediment, \*Limnol.\*](#)  
5 [Oceanogr., 51, 1557-1571, 2006.](#)
- 6 Kristensen, E., Bouillon, S., Dittmar, T., and Marchand, C.: Organic carbon dynamics in  
7 mangrove ecosystems: a review, *Aquat. Bot.*, 89, 201–219, 2008.
- 8 [Lee, R., Porubsky, W., Feller, I., McKee, K., and Joye, S.: Porewater biogeochemistry and soil](#)  
9 [metabolism in dwarf red mangrove habitats \(Twin Cays, Belize\), \*Biogeochemistry\*, 87,](#)  
10 [181-198, 2008.](#)
- 11 Lee, S. Y.: Mangrove outwelling – a review, *Hydrobiologia*, 295, 203–212, 1995.
- 12 Lekphet, S., Nitisoravut, S., and Adsavakulchai, S.: Estimating methane emissions from  
13 mangrove area in Ranong Province, Thailand, *Songklanakarin, J. Sci. Technol.*, 27, 153–163,  
14 2005.
- 15 Linto, N., Barnes, J., Ramachandran, R., Divia, J., Ramachandran, P., and Upstill-Goddard, R.  
16 C.: Carbon dioxide and methane emissions from mangrove-associated waters of the Andaman  
17 islands, Bay of Bengal, *Estuar. Coast.*, 37, 381–398, 2014.
- 18 Lyimo, T. J., Pol, A., den Camp, H. J. M., Harhangi, H. R., and Vogels, G. D.: *Methanosarcina*  
19 *semesiae* sp nov., a dimethylsulfide-utilizing methanogen from mangrove sediment, *Int. J. Syst.*  
20 *Evol. Micr.*, 50, 171–178, 2000.
- 21 [Maltby, J., Sommer, S., Dale, A. W., and Treude, T.: Microbial methanogenesis in the](#)  
22 [sulfate-reducing zone of surface sediments traversing the Peruvian margin, \*Biogeosciences\*, 13,](#)  
23 [283-299, 2016.](#)
- 24 Martens, C. S. and Klump, V. J.: Biogeochemical cycling in an organic-rich coastal marine  
25 basin. I. Methane sediment-water exchange processes, *Geochim. Cosmochim. Ac.*, 44, 471–490,  
26 1980.
- 27 Martens, C. S. and Klump, V. J.: Biogeochemical cycling in an organic-rich coastal marine  
28 basin 4. An organic carbon budget for sediments dominated by sulfate reduction and  
29 methanogenesis, *Geochim. Cosmochim. Ac.*, 48, 1987–2004, 1984.
- 30 [Mitsch, W.J., Gosselink, J.G.: \*Wetlands\*. Wiley, New York, p. 936, 2000.](#)
- 31 Mohanraju, R., Rajagopal, B. S., and Daniels, L.: Isolation and characterization of a  
32 methanogenic bacterium from mangrove sediments, *J. Mar. Biotechnol.*, 5, 147–152, 1997.

1 Odum, W. E. and Heald, E. J.: The detritus-based food web of an estuarine mangrove  
2 community, in: Estuarine Research, edited by: Cronin, L. E., New York, Academic Press, Inc.,  
3 265–286, 1975.

4 Oremland, R. S. and Polcin, S.: Methanogenesis and sulfate reduction – competitive and non  
5 competitive substrates in estuarine sediments, *Appl. Environ. Microb.*, 44, 1270–1276, 1982.

6 Perry, E., Velazquez-Oliman, G., and Marin, L.: The hydrogeochemistry of the karst aquifer  
7 system of the northern Yucatan Peninsula, Mexico, *Int. Geol. Rev.*, 44, 191–221, 2002.

8 Perry, E., Paytan, A., Pedersen, B., and Velazquez-Oliman, G.: Groundwater geochemistry of  
9 the Yucatan Peninsula, Mexico: constraints on stratigraphy and hydrogeology, *J. Hydrol.*, 367,  
10 27–40, 2009.

11 Pilson, M. E. Q.: *An Introduction to the Chemistry of the Sea*, Prentice Hall, Upper Saddle  
12 River, New Jersey, 431 pp., 1998.

13 [Poulton, Simon, W., Canfield, and Donald, E.: Development of a sequential extraction](#)  
14 [procedure for iron: implications for iron partitioning in continentally derived particulates.](#)  
15 [Elsevier B.V., 2005.](#)

16 Purvaja, R. and Ramesh, R.: Human impacts on methane emission from mangrove ecosystems  
17 in India, *Reg. Environ. Change*, 1, 86–97, 2000.

18 Purvaja, R. and Ramesh, R.: Natural and anthropogenic methane emission from coastal  
19 wetlands of South India, *Environ. Manage.*, 27, 547–557, 2001.

20 [Raghoebarsing, A. A., Pol, A., van de Pas-Schoonen, K. T., Smolders, A. J. P., Ettwig, K. F.,](#)  
21 [Rijpstra, W. I. C., Schouten, S., Damste, J. S. S., Op den Camp, H. J. M., Jetten, M. S. M., and](#)  
22 [Strous, M.: A microbial consortium couples anaerobic methane oxidation to denitrification,](#)  
23 [Nature, 440, 918-921, 2006.](#)

24 Ramesh, R., Purvaja, G. R., Parashar, D. C., Gupta, P. K., and Mitra, A. P.: Anthropogenic  
25 forcing on methane e<sub>ux</sub> from polluted wetlands (Adyar River) of Madras City, India, *Ambio*,  
26 26, 369–374, 1997.

27 Ramesh, R., Purvaja, R., Neetha, V., Divia, J., Barnes, J., and Upstill-Goddard, R.: CO<sub>2</sub> and  
28 CH<sub>4</sub> emissions from Indian mangroves and its surrounding waters, in: *Greenhouse gas and*  
29 *carbon balances in mangrove coastal ecosystems*, Proceedings, edited by: Tateda, Y., Gendai  
30 Tosho, Kanagawa, Japan, 153–164, 2007.

31 [Segarra, K. E. A., Comerford, C., Slaughter, J., and Joye, S. B.: Impact of electron acceptor](#)  
32 [availability on the anaerobic oxidation of methane in coastal freshwater and brackish wetland](#)

**Deleted:** Regnier, P., Dale, A. W., Arndt, S., LaRowe, D. E., Mogollon, J., and Van Cappellen, P.: Quantitative analysis of anaerobic oxidation of methane (AOM) in marine sediments: a modeling perspective, *Earth-Sci. Rev.*, 106, 105–130, 2011.

1 [sediments, \*Geochimica et Cosmochimica Acta\*, 115, 15-30, 2013.](#)

2 [Segarra, K. E. A., Schubotz, F., Samarkin, V., Yoshinaga, M. Y., Hinrichs, K. U., and Joye, S.](#)  
3 [B.: High rates of anaerobic methane oxidation in freshwater wetlands reduce potential](#)  
4 [atmospheric methane emissions, \*Nat Commun\*, 6, 2015.](#)

5 [Sivan, O., Adler, M., Pearson, A., Gelman, F., Bar-Or, I., John, S. G., and Eckert, W.:](#)  
6 [Geochemical evidence for iron-mediated anaerobic oxidation of methane, \*Limnol. Oceanogr.\*,](#)  
7 [56, 1536-1544, 2011.](#)

8 Sotomayor, D., Corredor, J. E., and Morell, J. M.: Methane flux from mangrove sediments  
9 along the southwestern coast of Puerto-Rico, *Estuaries*, 17, 140–147, 1994.

10 [Taketani, R., Yoshiura, C., Dias, A., Andreote, F., and Tsai, S.: Diversity and identification of](#)  
11 [methanogenic archaea and sulphate-reducing bacteria in sediments from a pristine tropical](#)  
12 [mangrove, \*Antonie van Leeuwenhoek\*, 97, 401-411, 2010.](#)

13 [Thalasso, F., Vallecillo, A., García-Encina, P., and Fdz-Polanco, F.: The use of methane as a](#)  
14 [sole carbon source for wastewater denitrification, \*Water Research\*, 31, 55-60, 1997.](#)

15 [Torres-Alvarado, M., José Fernández, F., Ramírez Vives, F., and Varona-Cordero, F.: Dynamics](#)  
16 [of the methanogenic archaea in tropical estuarine sediments, \*Archaea\*, 13, 582646,](#)  
17 [doi:10.1155/2013/582646, 2013.](#)

18 Valdes, D. S. and Real, E.: Variations and relationships of salinity, nutrients and suspended  
19 solids in Chelem coastal lagoon at Yucatan, Mexico, *Indian J. Mar. Sci.*, 27, 149–156, 1998.

20 Valentine, D. L. and Reeburgh, W. S.: New perspectives on anaerobic methane oxidation,  
21 *Environ. Microbiol.*, 2, 477–484, 2000.

22 Verma, A., Subramanian, V., and Ramesh, R.: Day-time variation in methane emission from  
23 two tropical urban wetlands in Chennai, Tamil Nadu, India, *Curr. Sci. India*, 76, 1020–1022,  
24 1999.

25 Wallmann, K., Aloisi, G., Haeckel, M., Obzhairov, A., Pavlova, G., and Tishchenko, P.: Kinetics  
26 of organic matter degradation, microbial methane generation, and gas hydrate formation in  
27 anoxic marine sediments, *Geochim. Cosmochim. Ac.*, 70, 3905–3927, 2006.

28 Wellsbury, P. and Parkes, R. J.: Deep biosphere: source of methane for oceanic hydrate, in:  
29 *Natural gas hydrate in oceanic and permafrost environments*, edited by: Max, M. D., Springer,  
30 New York, 91–104, 2000.

31 [Weston, N., Vile, M., Neubauer, S., and Velinsky, D.: Accelerated microbial organic matter](#)  
32 [mineralization following salt-water intrusion into tidal freshwater marsh soils, \*Biogeochemistry\*,](#)

Deleted: -

1 [102, 135-151, 2011.](#)

2 Whalen, S. C.: Biogeochemistry of methane exchange between natural wetlands and the  
3 atmosphere, *Environ. Eng. Sci.*, 22, 73–94, 2005.

4 Young, M. B., Gonneea, M. E., Herrerasilveira, J. A., and Paytan, A.: Export of Dissolved and  
5 Particulate Carbon and Nitrogen From a Mangrove-Dominated Lagoon, Yucatán Peninsula,  
6 Mexico, *Int. J. Ecol. Environ. Sci.*, 31, 189–202, 2005.

7 Young, M. B., Gonneea, M. E., Fong, D. A., Moore, W. S., Herrera-Silveira, J., and Paytan, A.:  
8 Characterizing sources of groundwater to a tropical coastal lagoon in a karstic area using  
9 radium isotopes and water chemistry, *Mar. Chem.*, 109, 377–394, 2008.

10

1 Table 1: Experimental conditions and sampling time intervals for methane headspace  
 2 concentration analysis of sediment slurry incubations.  
 3

	Treatment	Initial concentration of treatment	Experiment length (days)	Number of measurements	Methane production rate (nmol CH <sub>4</sub> cm <sup>-3</sup> slurry d <sup>-1</sup> )
Controls	No amendment (anaerobic)	N <sub>2</sub> headspace	29	3	1.3 × 10 <sup>-4</sup> to 2.0 × 10 <sup>-3</sup>
	Autoclaved	N <sub>2</sub> headspace	29	3	0 to 2.6 × 10 <sup>-3</sup>
	Aerobic- O <sub>2</sub> gas	16% O <sub>2</sub> headspace (0.36 mM)	29	3	5.7 × 10 <sup>-4</sup> to 3.5 × 10 <sup>-3</sup>
		BES	40 mM	29	3
Competitive substrates	H <sub>2</sub> gas	100% headspace (1.8 mM)	29	3	5.4 × 10 <sup>-3</sup> to 6.2
	Acetate	10 mM	29	3	6.8 × 10 <sup>-4</sup> to 9.2 × 10 <sup>-2</sup>
	Formate	10 mM	29	3	6.9 × 10 <sup>-4</sup> to 1.6 × 10 <sup>-1</sup>
Noncompetitive substrates	Methanol	10 mM	29	4	2.0 × 10 <sup>-2</sup> to 19
	TMA	10 mM	29	4	5.4 × 10 <sup>-4</sup> to 40

4

1 **Table 2.** Model-derived depth-integrated turnover rates ( $\text{mmol m}^{-2} \text{d}^{-1}$ ), dissolved methane fluxes to the water column ( $\text{mmol m}^{-2} \text{d}^{-1}$ ) and contributions of  
2 methanogenesis to net methane production (%) and heterotrophic sulfate reduction to POC degradation (%). CEL and CH represent cores collected from  
3 Celestún Lagoon and Chelem Lagoon.

	Length of model column (cm)	$R_{SD}$ = $R_{SR}$	$R_M$	$R_{POC}$	$R_{MB}$	$F_{methane (top)}$	$F_{methane (bottom)}$	$R_M/(R_M+R_{MB})$	$2R_{SR}/R_{POC}$	$F_{SO_4^{2-}}$	$F_{CH_4}$
Group-1											
1CEL_Apr00	20	3.7	0.13	7.7	0.41	0.59	0.06	25%	97%		
1CEL_Dec00	20	2.2	1.5	7.4	0	0.94	-0.60	100%	59%		
1CEL_Oct01	20	6.2	0.12	13	0.32	0.40	-0.04	27%	98%		
1CEL_Jul02	20	3.6	8.0	23	0	6.0	-1.98	100%	31%		
2CEL_Dec00	20	1.1	0.05	2.3	0.76	0.54	-0.27	5.8%	96%		
2CEL_Jul02	20	11	0.08	22	0.05	0.11	-0.02	63%	99%		
3CEL_Apr00	20	1.3	0.29	3.2	0.24	0.68	0.15	55%	82%		
3CEL_Jul02	20	7.1	0.25	15	2.2	3.0	0.63	10%	97%		
1_1CH_Oct01	13.75	24	31	110	0	11	-19.54	100%	42%		
1_2CH_Oct01	20	3.0	26	58	0	20	-5.6	100%	10%		
Group-2											
1CH_Dec00	20					0.52	-7.0			4.5	7.8
1CH_Apr00	20					~0	~0			-3.2	~0
2CH_Dec00	20					~0	~0			6.9	~0
5CH_Apr00	20					0.012	~0			21	0.013
2CEL_Oct01	20					11	-0.01			3.9	11
14CEL_Jul02	20					0.27	~0			3.7	0.27
16CEL_Dec00	20					-0.047	0.013			-1.8	-0.060
Group-3											
5CEL_Apr00	10					0.014	-0.01			-69	0.028
14CEL_Dec00	20					3.4	-0.13			10	3.6
14CEL_Oct01	20					0.088	-0.01			2.9	0.10
Group-4											
16CEL_Jul02	20					0.096	0.02			6.1	0.072
16CEL_Oct01	20					~0	~0			0.83	~0
7CH_Oct01	20					0.13	~0			2.6	0.14
8CH_Dec00	20					~0	~0			0.85	0.012

4  $R_{SD}$  is net sulfate depletion ( $\text{mmol m}^{-2} \text{d}^{-1}$  of  $\text{SO}_4^{2-}$ ).  $R_{SR}$  is heterotrophic sulfate reduction ( $\text{mmol m}^{-2} \text{d}^{-1}$  of  $\text{SO}_4^{2-}$ ).  $R_M$  is methanogenesis rate ( $\text{mmol m}^{-2} \text{d}^{-1}$  of  $\text{CH}_4$ ).  $R_{POC}$  is total POC mineralization  
5 ( $\text{mmol m}^{-2} \text{d}^{-1}$  of C).  $R_{MB}$  is gas dissolution ( $\text{mmol m}^{-2} \text{d}^{-1}$  of  $\text{CH}_4$ ).  $F_{methane (top)}$  is methane flux across the sediment surface ( $\text{mmol m}^{-2} \text{d}^{-1}$  of  $\text{CH}_4$ ). Negative values in  $F_{methane (top)}$  represent methane flux  
6 into the sediments from the water column and vice versa.  $F_{methane (bottom)}$  is the methane flux across the 20cm lower boundary ( $\text{mmol m}^{-2} \text{d}^{-1}$  of  $\text{CH}_4$ ). Negative values in  $F_{methane (bottom)}$  represent methane  
7 flux to deep sediments and vice versa.  $R_{SO_4^{2-}}$  is net sulfate input ( $\text{mmol m}^{-2} \text{d}^{-1}$  of  $\text{SO}_4^{2-}$ ) and  $R_{CH_4}$  is net methane production ( $\text{mmol m}^{-2} \text{d}^{-1}$  of  $\text{CH}_4$ ) for cores in group-2 to group-4. See Appendix for  
8 further model details.

1 Table 3: Maximum model-derived rates of methanogenesis and sulfate reduction for cores in  
 2 Group-1 and maximum model-derived rates of methane production and sulfate consumption  
 3 for cores in Group-2, Group-3 and Group-4. CEL and CH represent cores collected from  
 4 Celestún Lagoon and Chelem Lagoon.

	Max- $R_M$ (nmol CH <sub>4</sub> cm <sup>-3</sup> d <sup>-1</sup> )	Max- $R_{SR}$ (nmol SO <sub>4</sub> <sup>2-</sup> cm <sup>-3</sup> d <sup>-1</sup> )
Group-1		
1CEL_Apr00	9.0	304
1CEL_Dec00	116	559
1CEL_Oct01	7.1	740
1CEL_Jul02	564	1425
2CEL_Dec00	4.9	587
2CEL_Jul02	7.4	1323
3CEL_Apr00	20	405
3CEL_Jul02	26	1227
1_1CH_Oct01	2199	1802
1_2CH_Oct01	1959	1476
Group-2		
1CH_Dec00	2531	407
1CH_Apr00	1.6	2687
2CH_Dec00	1.1	2835
5CH_Apr00	2.1	8378
2CEL_Oct01	504	715
14CEL_Jul02	19	394
16CEL_Dec00	2.7	330
Group-4		
5CEL_Apr00	63	5212
14CEL_Dec00	1517	1756
14CEL_Oct01	23	1007
Group-5		
16CEL_Jul02	10	186
16CEL_Oct01	0.08	599
7CH_Oct01	4.1	940
8CH_Dec00	0.57	230

5

1 Table A1: Rate expressions applied in the differential equations ( $R_C$  in Eq. (2))

2

Variable	Rates	Applied cores
$\text{SO}_4^{2-}$	$-R_{SR}$	Group-1
$\text{CH}_4$	$+R_M + R_{MB}$	Group-1
$\text{SO}_4^{2- \text{dep}}$	$+R_{SD}$	Group-1
$\text{SO}_4^{2-}$	$+R_{\text{SO}_4^{2-}}$	Group-2, Group-3 and Group-4
$\text{CH}_4$	$+R_{\text{CH}_4}$	Group-2, Group-3 and Group-4

3

1 Table A2: Boundary conditions used in the model

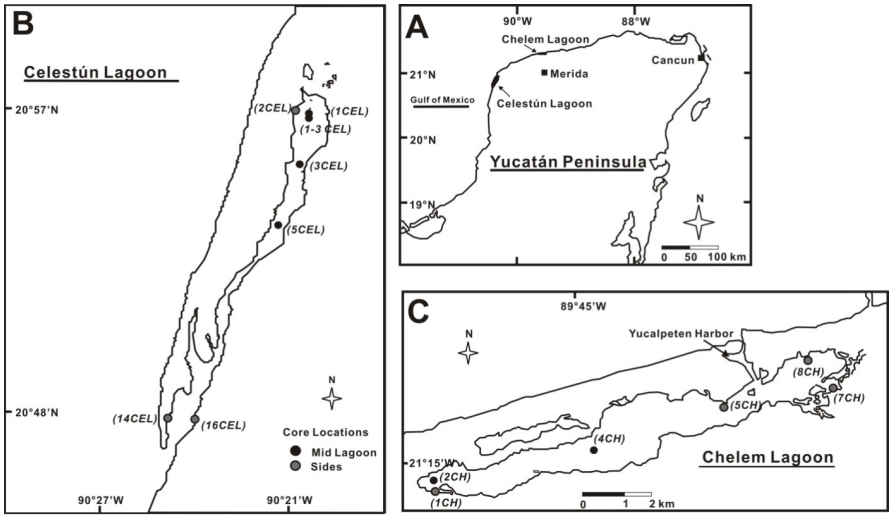
	SO <sub>4</sub> <sup>2-</sup> (top)	CH <sub>4</sub> (top)	SO <sub>4</sub> <sup>2-</sup> <sub>dep</sub> (top)	SO <sub>4</sub> <sup>2-</sup> (bottom)	CH <sub>4</sub> (bottom)	SO <sub>4</sub> <sup>2-</sup> <sub>dep</sub> (bottom)	Unit
Group-1							
1CEL_Apr00	5	0	4.8	8.5	0.5	5.534	mM
1CEL_Dec00	15	0.16	-2.2	5	0.56	2	mM
1CEL_Oct01	15	0	-2.3	7.5	0.295	4.6	mM
1CEL_Jul02	15	0.1	2.5	7.8	0.35	5.368	mM
2CEL_Jul02	18	0.02	10 <sup>-9</sup>	18.5	0.035	-2	mM
3CEL_Apr00	6.5	0.25	6.7	3.5	0.825	5.766	mM
3CEL_Jul02	13.8	0.31	2	6.5	1.3	3.5	mM
1_1CH_Oct01	15.1	0	12.4	13.2	0.0295	12.03	mM
1_2CH_Oct01	12	0.01	16	10	1	14.641	mM
2CEL_Dec00	21	0.01	-6.4451	7.6	0.25	4.6	mM
Group-2							
1CH_Dec00	11.5	0.102		9.2	0.522		mM
1CH_Apr00	32	0.005		12.5	0.006		mM
2CH_Dec00	19.9	0.0015		7.96	0.0019		mM
5CH_Apr00	31.7	0.0031		29.1	0.0145		mM
2CEL_Oct01	5.0	0.511		7.88	0.734		mM
14CEL_Jul02	18.3	0.085		31.5	0.02		mM
16CEL_Dec00	8.8	0.038		8.81	0.025		mM
Group-3							
5CEL_Apr00	17	0.047		11.6	0.0275		mM
14CEL_Dec00	20.5	2.1		34.9	0		mM
14CEL_Oct01	20	0.01		33	0.012		mM
Group-4							
16CEL_Jul02	21	0		25.65	0.070		mM
16CEL_Oct01	23	0.00139		25.8	0.0015		mM
7CH_Oct01	20.5	0.00477		19.1	0.01		mM
8CH_Dec00	18.6	0		19	0.013		mM

2

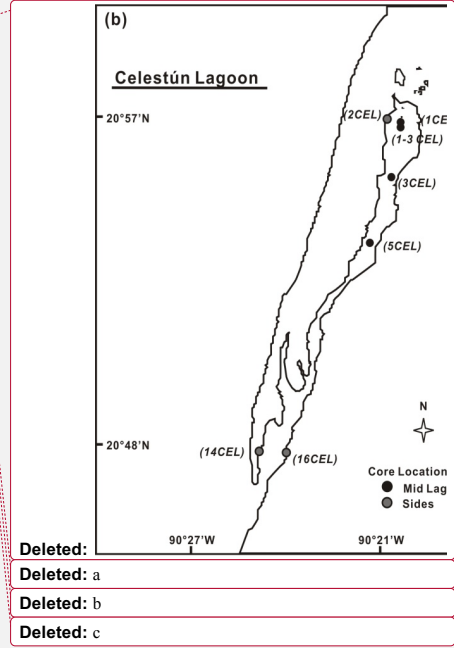
1 Table A3: Imposed and best-fit parameters in each core

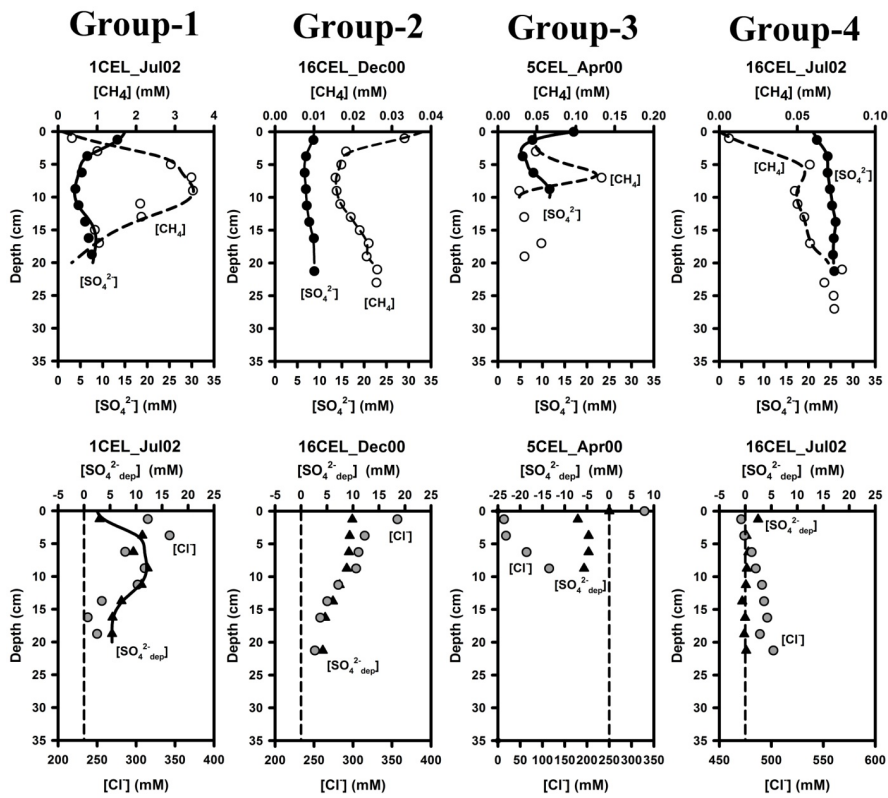
2

	T	S	P	$D_{m(SO_4^{2-})}$	$D_{m(CH_4)}$	$D_{m(SO_4^{2-}dep)}$	$L_{MB}$	$k_{MB}$	$k_{SD}$	$k_{CH_4}$	$k_{SO_4^{2-}}$
	(°C)	(-)	(bar)	( $cm^2 yr^{-1}$ )	( $cm^2 yr^{-1}$ )	( $cm^2 yr^{-1}$ )	(mM)	( $yr^{-1}$ )	( $yr^{-1}$ )	( $yr^{-1}$ )	( $yr^{-1}$ )
1CEL_Apr00	27.3	17.6	1.06	354	598	354	1.2	1	500		
1CEL_Dec00	22.2	16.4	1.06	367	523	367	1.3	0	400		
1CEL_Oct01	31.2	13.9	1.1	382	659	382	1.36	0.6	500		
1CEL_Jul02	30	21.1	1.01	374	640	374	1.1	0	500		
2CEL_Dec00	22	17.7	1.06	315	520	315	1.31	1.6	500		
2CEL_Jul02	28.7	20.8	1.01	364	619	364	1.12	0.1	500		
3CEL_Apr00	28.6	20.2	1.07	363	618	363	1.19	0.9	400		
3CEL_Jul02	30.4	18.2	1.01	377	646	377	1.09	50	500		
1_1CH_Oct01	29.8	32.1	1.01	372	636	372	1.1	0	500		
1_2CH_Oct01	29.8	32.1	1.01	372	636	372	1.1	0	500		
Group-2											
1CH_Dec00	25.2	24.8	1.05	318	526					1000	300
1CH_Apr00	26.3	39.4	1.09	347	583					1000	500
2CH_Dec00	23.9	27.5	1.08	329	547					4000	2000
5CH_Apr00	29.6	38	1.04	382	659					1000	1000
2CEL_Oct01	31.2	14.3	1.1	382	659					1000	500
14CEL_Jul02	31.5	27.4	1.01	385	663					1000	300
16CEL_Dec00	22.6	31.2	1.02	319	529					1000	300
Group-3											
5CEL_Apr00	26.5	21.1	1.06	348	586					1100	3000
14CEL_Dec00	23.5	31.1	1.06	326	541					1000	300
14CEL_Oct01	31.1	13.9	1.07	382	657					1000	500
Group-4											
16CEL_Jul02	30.3	30.5	1.01	376	644					600	300
16CEL_Oct01	29.7	28.2	1.06	319	529					1000	300
7CH_Oct01	29.6	31.3	1.01	371	633					500	300
8CH_Dec00	24.4	31.3	1.05	333	555					500	300



1  
 2 Figure 1: Maps of (A) the Yucatán Peninsula with lagoon locations, (B) Celestún Lagoon and  
 3 (C) Chelem Lagoon showing the sampling stations (circles) of sediment cores.  
 4

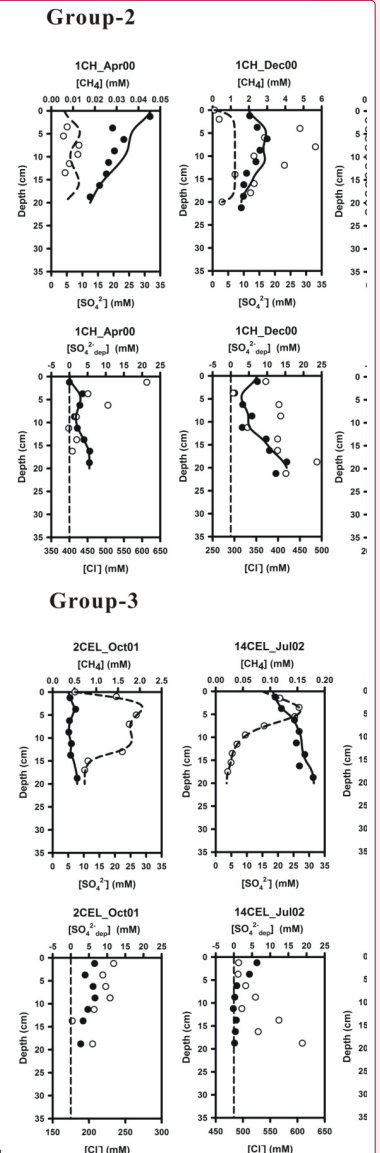




1  
 2 Figure 2: Depth profiles of modeled (lines) and measured (circles) and calculated (triangles)  
 3 concentration of dissolved methane (dashed lines; open circles), sulfate (solid lines; solid  
 4 circles) in the upper panel and sulfate depletion (solid lines; solid circles), zero sulfate  
 5 depletion (dashed lines) and chloride concentration (gray circles) in the lower panel for each  
 6 profile type (Groups 1-4, see text). One selected profile per group is shown here for illustration  
 7 and the other profiles for each group (9 cores for Group-1, 6 cores for Group-2, 2 cores for  
 8 Group-3 and 3 cores for Group-4) are presented in the Appendix (Fig. A1). CEL and CH  
 9 represent cores collected from Celestún Lagoon and Chelem Lagoon.

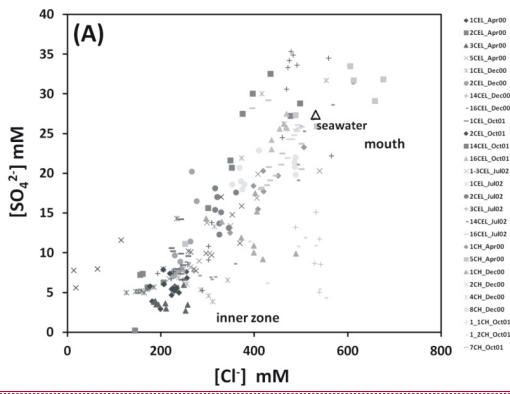
Deleted: <sp>

Deleted: /calculated...(circlessymbols... and calcula... [11]

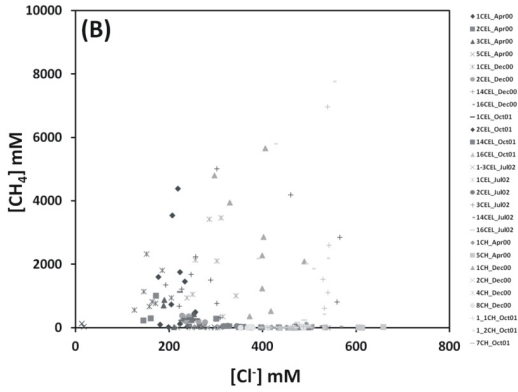


Deleted:

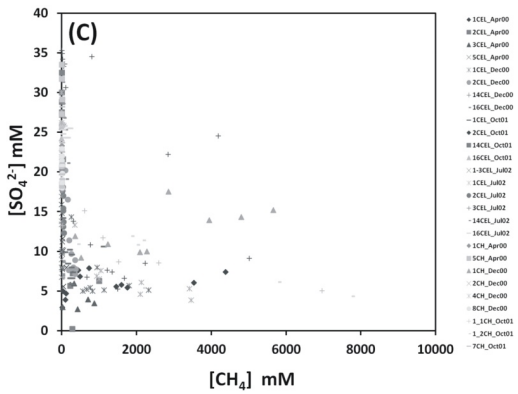
Deleted: ... [12]



1



2



3

4 Figure 3: Relationship between (A)  $[Cl^-]$  and  $[SO_4^{2-}]$ , (B)  $[Cl^-]$  and  $[CH_4]$  and (C) relationship  
 5  $[CH_4]$  and  $[SO_4^{2-}]$  in porewater samples.

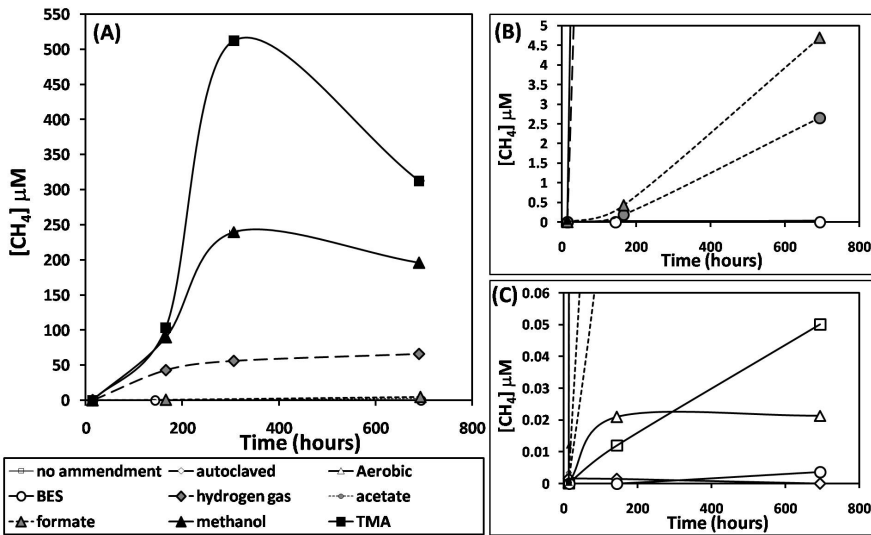
Deleted: (A) - ... [13]

Deleted: (A)

Deleted: relationship between

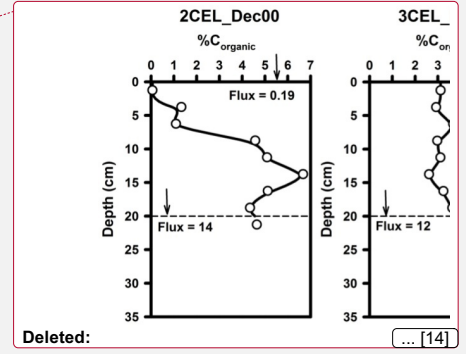
Deleted: between

1



2

3 Figure 4: (A) Headspace methane concentrations in sediment slurry incubations. (B) Expansion  
 4 of (A), showing results for acetate, formate, and controls. (C) Expansion of (A), showing  
 5 results for controls only. Error bars represent one standard deviation for triplicate sample  
 6 bottles.

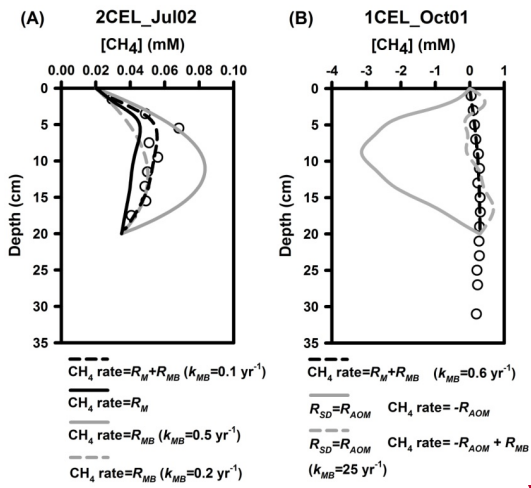


Deleted:

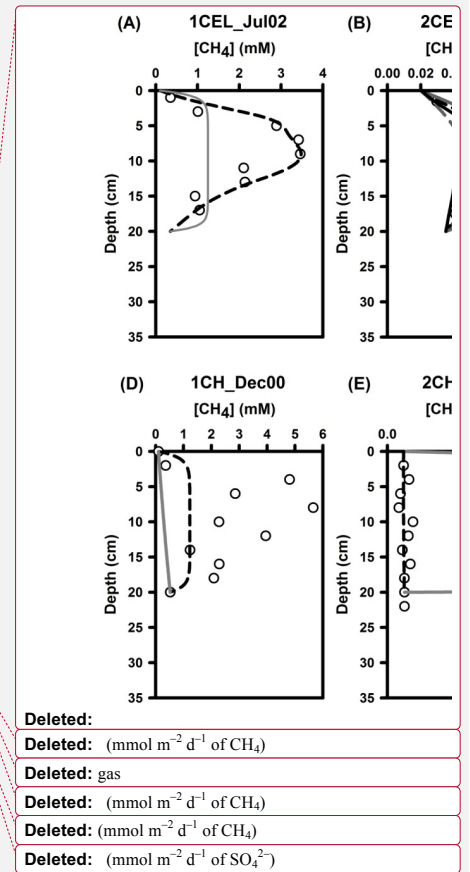
[14]

Deleted: 5

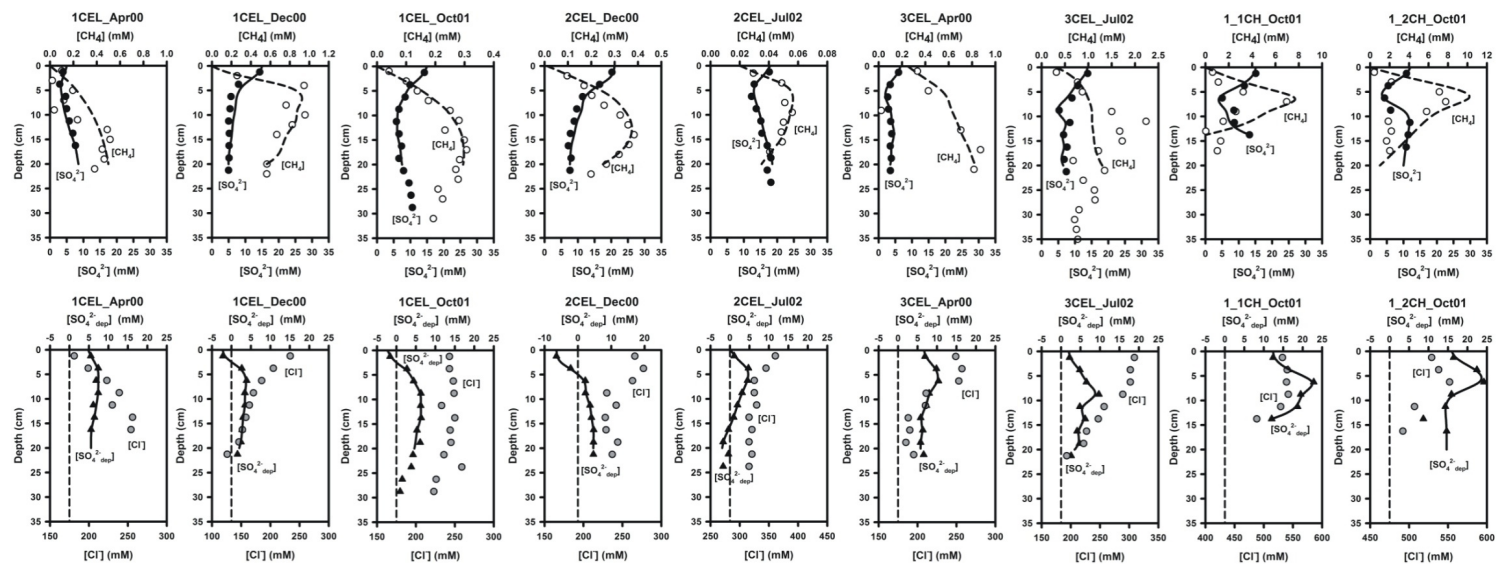
Deleted: CH<sub>4</sub>



1  
2 Figure 5: Model sensitivity analysis of methane concentrations for cores in Group-1 to  
3 the different processes controlling methane concentrations in porewaters. Black dashed  
4 lines denote the standard simulation results: CH<sub>4</sub> production rate = +  $R_{MB}$  +  $R_M$ .  $R_M$  is  
5 methanogenesis,  $R_{MB}$  is methane bubble dissolution,  $R_{AOM}$  is anaerobic oxidation of  
6 methane and  $R_{SD}$  is net sulfate depletion.



## Group-1

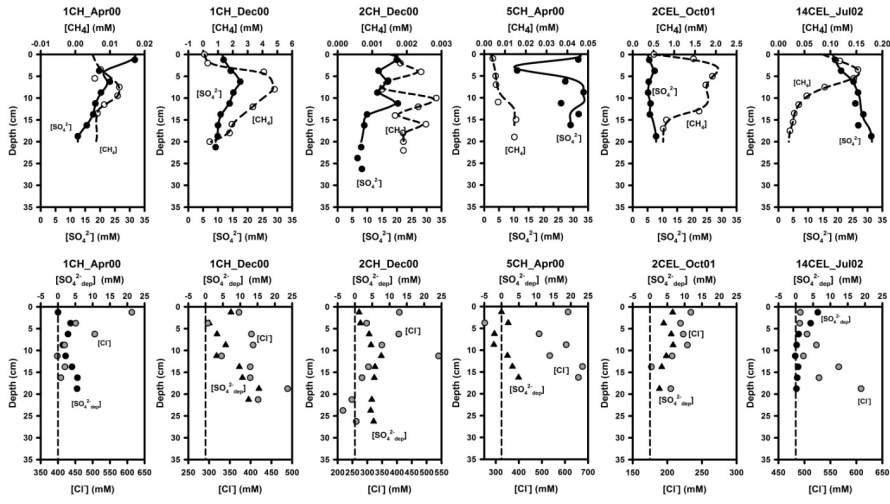


1  
2 Figure A1: Depth profiles of modeled (lines), measured (circles) and calculated (triangles) concentration of dissolved methane (dashed lines; open  
3 circles), sulfate (solid lines; solid circles) in the upper panel and sulfate depletion (solid lines; solid triangles), zero sulfate depletion (dashed lines) and  
4 chloride (gray circles) in the lower panel for each profile type (Groups 1-4, see text). One selected profile per group is shown in Fig. 2 for illustration  
5 and here the rest of other profiles are shown (9 cores for Group-1, 6 cores for Group-2, 2 cores for Group-3 and 3 cores for Group-4). CEL and CH  
6 represent cores collected from Celestún Lagoon and Chelem Lagoon.

Deleted: are

Deleted: the

Group-2

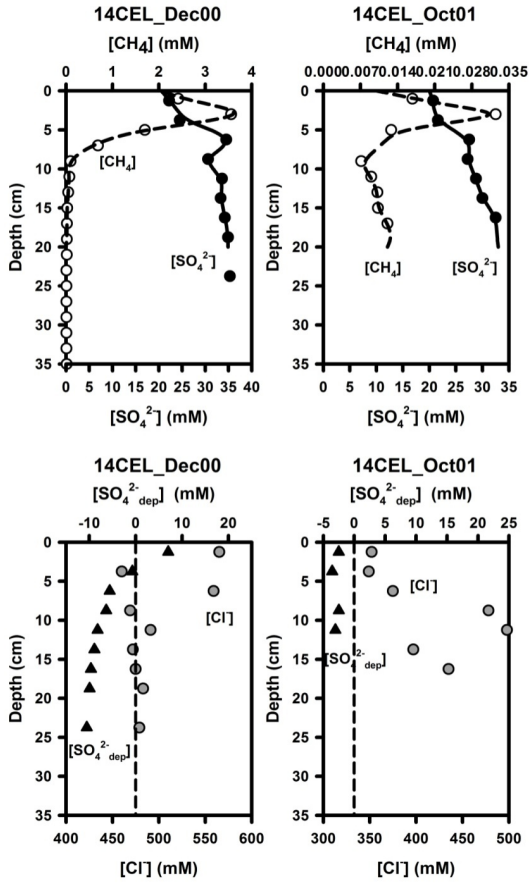


- 1
- 2
- 3
- 4

Figure A1: Continued.

1

# Group-3

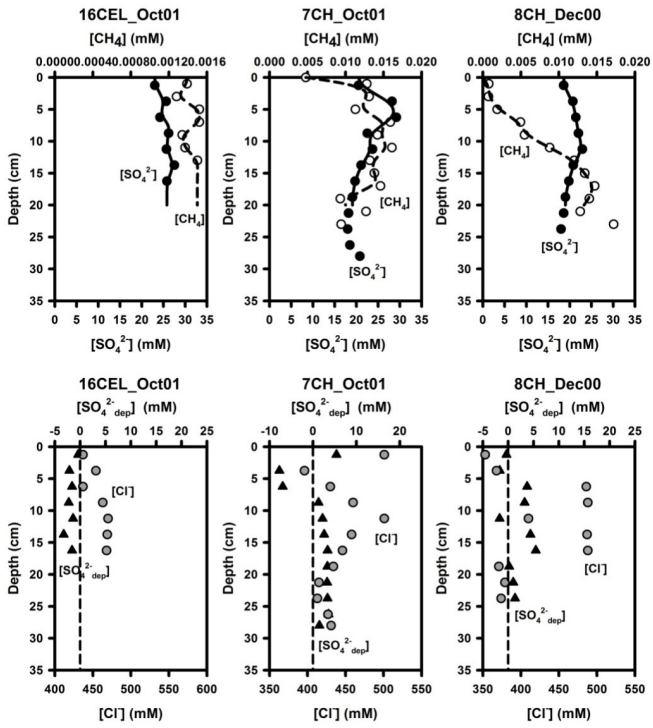


2

3 [Figure A1: Continued.](#)

4

# Group-4



- 1
- 2
- 3
- 4
- 5

Figure A1: Continued.

**Deleted:** Figure 6: Sensitivity of methane concentrations for cores in group-1 and group-2 to the different processes: (A)  $R_{CH_4} = -R_{AOM} + R_{MB}$  (gray solid line;  $k_{MB} = 1000 \text{ yr}^{-1}$ ), (B)  $R_{CH_4} = -R_{AOM} + R_{MB}$  (gray solid line;  $k_{MB} = 0.5 \text{ yr}^{-1}$ ),  $R_{CH_4} = -R_{AOM} + R_{MB}$  (gray dashed line;  $k_{MB} = 0.2 \text{ yr}^{-1}$ ) and  $R_{CH_4} = -R_{AOM} + R_M$  (black solid line), (C)  $R_{CH_4} = -R_{AOM} + R_M$  (gray solid line), (D)  $R_{CH_4} = -R_{AOM}$  (gray solid line), (E)  $R_{CH_4} = -R_{AOM} + R_M$  (gray solid line), (F)  $R_{CH_4} = -R_{AOM} + R_M$  (gray solid line). Black dashed curves denote the standard simulation results: (A)  $R_{CH_4} = -R_{AOM} + R_M$  and (B)  $R_{CH_4} = -R_{AOM} + R_{MB} + R_M$  ( $k_{MB} = 0.1 \text{ yr}^{-1}$ ).